Computers and Chemical Engineering 74 (2015) 184–203

Contents lists available at ScienceDirect

Computers and Chemical Engineering

journal homepage: www.elsevier.com/locate/compchemeng

Municipal solid waste to liquid transportation fuels – Part II: Process synthesis and global optimization strategies

Alexander M. Niziolek, Onur Onel, M.M. Faruque Hasan, Christodoulos A. Floudas*

Department of Chemical and Biological Engineering, Princeton University, Princeton, NJ 08544, USA

ARTICLE INFO

Article history:
Received 18 June 2014
Received in revised form 6 October 2014
Accepted 14 October 2014
Available online 27 October 2014

Keywords:
Municipal solid waste
Process synthesis
Global optimization
Mathematical modeling
Mixed-integer nonlinear optimization

ABSTRACT

This paper investigates the production of liquid transportation fuels from municipal solid waste (MSW). A comprehensive process synthesis superstructure is utilized that incorporates a novel mathematical model for MSW gasification. The production of liquid products proceeds through a synthesis gas intermediate that can be converted into Fischer–Tropsch hydrocarbons or methanol. The methanol can be converted into either gasoline or olefins, and the olefins may subsequently be converted into gasoline and distillate. Simultaneous heat, power, and water integration is included within the process synthesis framework to minimize utilities costs. A rigorous deterministic global optimization branch-and-bound strategy is utilized to minimize the overall cost of the waste-to-liquids (WTL) refinery and determine the optimal process topology. Several case studies are presented to illustrate the process synthesis framework and the nonconvex mixed-integer nonlinear optimization model presented in this paper. This is the first study that explores the possibility of liquid fuels production from municipal solid waste utilizing a process synthesis approach within a global optimization framework. The results suggest that the production of liquid fuels from MSW is competitive with petroleum-based processes. The effect that the delivered cost of municipal solid waste has on the overall cost of liquids production is also investigated parametrically.

1. Introduction

Recent interest from academia, industry, and government agencies to develop processes that can produce liquid fuels from domestically available carbon sources has emerged largely due to the challenges facing the U.S. transportation sector. These challenges include uncertainty over the future price of crude oil, substantial greenhouse gas emissions from the production of liquid fuels, and political unrest in the Middle East, the largest exporter of crude oil in the world (EIA, 2012). The U.S. consumes an estimated 18.714 million barrels of petroleum-based products per day (MMBD) in 2014 (Energy Information Administration, 2014). The majority of this consumption is attributable to the U.S. transportation section, which consumes 8.282 MMBD of gasoline, 2.695 MMBD of diesel, and 1.372 MMBD of jet fuel (Energy Information Administration, 2014). Three feedstocks that have been touted as alternatives to petroleum and have received the majority of attention include coal, biomass, and natural gas. The key contributions in the production of liquid fuels from single and hybrid combinations of these feedstocks has been highlighted in our recent reviews (Floudas et al., 2012; Elia and Floudas, 2014). This paper addresses the aforementioned challenges by introducing a novel mathematical model for gasification in a thermochemical-based process superstructure utilizing a fourth type of feedstock: municipal solid waste (MSW) (Onel et al., 2014).

The amount of municipal solid waste generated in the United States has increased from 208.3 million tons in 1990 to over 250 million tons in 2011 (EPA, 2011). Paper and paperboard, plastics, food waste, yard trimmings, and metals are the main constituents of MSW (EPA, 2011). In 2011, 53.6% of MSW was discarded in landfills, 34.7% was recycled, and 11.7% was combusted to recover energy (EPA, 2011). In 2010, there were 86 active waste-to-energy plants that processed nearly 100,000 tons of MSW daily (Michaels, 2010). The most prominent reason why municipal solid waste is an attractive precursor to liquid transportation fuels can be attributed to its negative cost. Facilities normally receive a tipping fee, which varies between $24 and $70/ton in the U.S., to dispose of MSW (Valkenburg et al., 2009; Jones et al., 2009).

The presence of incombustibles, glass, and metals in MSW poses a serious challenge against the utilization of this feedstock. Typically, a physical separation system is included in order to remove these materials from municipal solid waste (Diaz et al., 1982; European Commission, 2003; Krieth, 1994; White et al., 2001). The physical separation increases the heating value of the feedstock

* Corresponding author. Tel.: +1 609 258 4595; fax: +1 609 258 0211.
E-mail address: floudas@titan.princeton.edu (C.A. Floudas).

http://dx.doi.org/10.1016/j.compchemeng.2014.10.007
0098-1354/

while simultaneously homogenizing the feed (Jones et al., 2009). The lower heating value of MSW is around 11.7 MMBtu/ton (EIA, 2007), while the heating value of the processed, homogenized feed is around 16.8 MMBtu/ton (Jones et al., 2009).

Utilizing MSW as a feedstock for the production of energy has been shown to mitigate the disposal problems associated with this feedstock and reduces the need for fossil fuel use (Ruth, 1998). The European Union legislation seeks to reduce landfilled municipal solid waste to 35% by 2020 (Stehlík, 2009). Additionally, it has been shown that combusting 1 metric ton of MSW negates the need of mining 0.25 tons of high quality U.S. coal or importing 1 barrel of oil (Psomopoulos et al., 2009). By utilizing municipal solid waste towards the production of energy, the methane emissions from landfills can be limited, the CO_2 emissions from fossil fuel combustion can be avoided, and the CO_2 emissions from metals production can be eliminated (Michaels, 2010). Previous work by Warren and El-Halwagi assessed the technical and economic feasibility of two process configurations for a plant producing liquid fuels from coal and municipal solid waste (Warren and El-Halwagi, 1996). Additional work investigated the MSW management system that took into account the technical and environmental issues associated with this feedstock (Santibañez-Aguilar et al., 2013). However, this is the first study that presents a complete superstructure for the production of liquid transportation fuels from municipal solid waste using our recently proposed novel mathematical gasification model (Onel et al., 2014).

The use of a large-scale nonconvex mixed-integer nonlinear optimization (MINLP) model that can efficiently determine the optimal process topology for liquid fuels production from many topological alternatives is described in this study. A rigorous global optimization branch-and-bound strategy is employed to mathematically guarantee that the value of the objective function (i.e., cost of liquid fuels production) is within a few percent of the best possible value (Baliban et al., 2012a). The production of liquid transportation fuels proceeds through a synthesis gas (syngas) intermediate that can be directed to either the Fischer–Tropsch refining or methanol conversion sections. The process synthesis superstructure utilizing coal, biomass, and/or natural gas as feedstocks has been described in previous works (Baliban et al., 2010, 2011, 2012a,b,c, 2013a,b,c,d,e; Elia et al., 2010; Niziolek et al., 2014); however, the following section will describe the key process units in the waste-to-liquids (WTL) refinery. An optimization-based heat-integration approach (Duran and Grossmann, 1986) is utilized to include simultaneous heat and power integration that can convert waste heat into electricity in the WTL refinery (Elia et al., 2010; Baliban et al., 2011). A wastewater-treatment section minimizes the amount of freshwater intake into the plant (Elia et al., 2010; Baliban et al., 2011; Karuppiah and Grossmann, 2006; Grossmann and Martín, 2010; Ahmetovic and Grossmann, 2010a,b). Finally, the life-cycle CO_2 emissions of the WTL plant are calculated and compared with petroleum-based processes.

The process synthesis framework for the WTL refinery includes (i) municipal solid waste gasification with/without recycle gas, (ii) syngas conversion via Fischer–Tropsch (FT) refining or methanol synthesis, (iii) methanol conversion via methanol-to-gasoline (MTG) or methanol-to-olefins (MTO), (iv) hydrocarbon upgrading via ZSM-5 zeolite catalysis, olefin oligomerization, or carbon number fractionation and subsequent treatment. The major liquid fuels products from the refinery include gasoline, diesel, and jet fuel, whereas liquefied petroleum gas (LPG) and electricity may be sold as byproducts.

2. WTL process superstructure: conceptual design and mathematical modeling

Previous studies by Baliban et al., Elia et al., and Niziolek et al., have detailed the conceptual design of refineries utilizing coal, biomass, and natural gas (Baliban et al., 2010, 2011, 2012a,b,c, 2013a,b,c,d,e; Elia et al., 2010; Niziolek et al., 2014). This section will outline the major components in the WTL refinery.

2.1. Municipal solid waste handling and gasification

2.1.1. Refuse derived fuel facility

Utilizing municipal solid waste as a potential feedstock for the production of liquid fuels has several challenges. In addition to the variabilities in the composition of the feedstock from location to location, there are undesired components (glass, metals, etc.) that can contaminate the gasifiers and downstream hydrocarbon production and upgrading reactors. Also, the moisture content is non-uniform among different types of municipal solid waste. To avoid these challenges, it is necessary to produce refuse derived fuel (RDF) from MSW before sending it to the gasifier. In the RDF facility, the MSW is converted into a higher-calorific fuel by removing the non-combustibles and recyclables. The RDF fuel leaving the RDF facility has a more consistent quality, composition, and moisture to avoid fluctuations caused by the variability in the inlet composition.

The municipal solid waste is delivered to the refinery gate and treated at the refuse derived fuel (RDF) facility, shown in Fig. 1. After the municipal solid waste is loaded onto a series of cranes and conveyors, the first step in the RDF facility is the reduction in size of the feedstock to liberate the composite material and meet the required dimensions for further processing (Christensen, 2011). The processed municipal solid waste is then sent to a magnetic separator and eddy current separator that remove the ferrous and nonferrous metals, respectively. Disc screens are then used

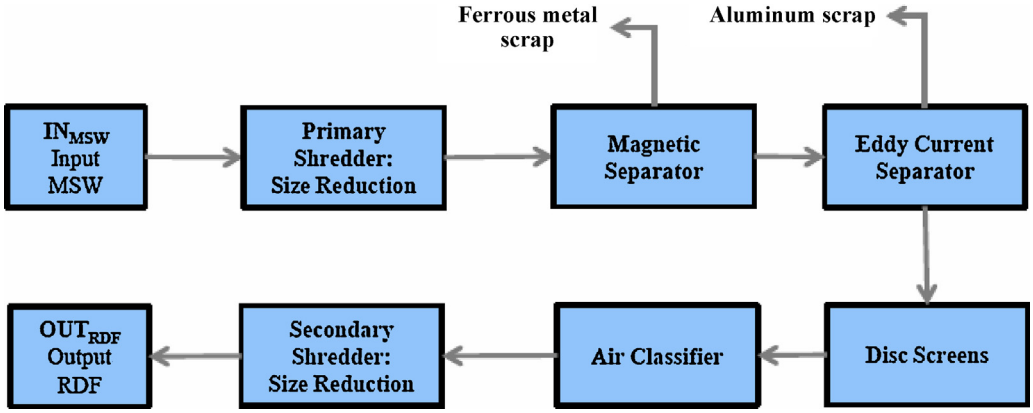

Fig. 1. Refuse derived fuel facility flow diagram. The municipal solid waste is converted into a higher-calorific fuel through removal of the non-combustibles and recyclables.

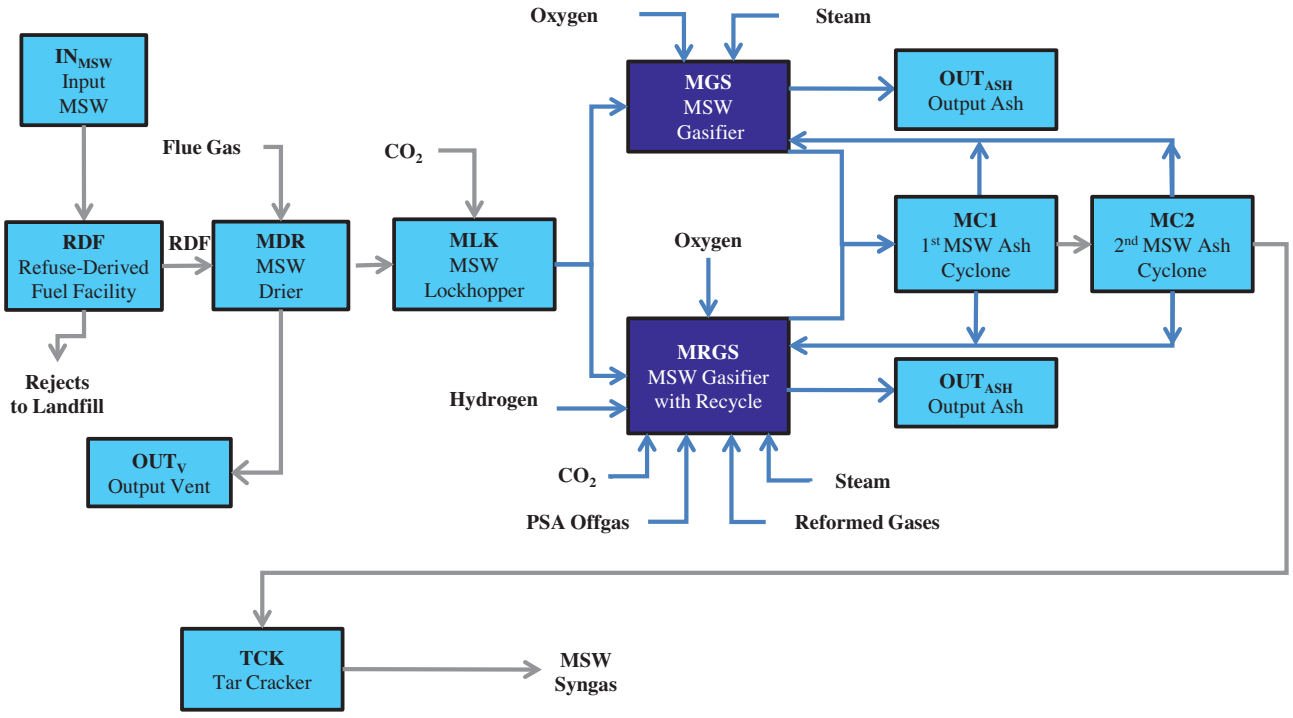

Fig. 2. Municipal solid waste gasification flow diagram. The municipal solid waste is first directed to the RDF facility. The RDF is then dried to 8.8 wt% moisture and transferred to one of two types of gasifiers via a lockhopper and compressed CO_2. The MSW gasifier can either operate with a solid feed (MSW) or with a solid/vapor feed (MSW/recycle gases). Any ash present within the MSW is ultimately output as slag. A catalytic tar cracker reforms the raw syngas before directing it to the syngas cleaning section.

to separate the feedstock by size. An air classification unit separates the feedstock by weight and recovers the high caloric fraction while reducing the ash content (Christensen, 2011). Finally, a secondary shredder creates a more uniform fuel that is ready to be processed in the refinery. The design of the RDF facility is based on one presented by the Pacific Northwest National Laboratory (Jones et al., 2009). The rejected material, which contains glass, dirt, and some combustible material, as well as the recovered scrap metal, is 20% of the MSW feed (Jones et al., 2009). The rejects and scrap metal are sent to the landfill. Most of the non-combustible material present in MSW is no longer present in RDF. In addition, the particle size, calorific content, water content, and ash content of the refuse derived fuel is more uniform than that of the unprocessed municipal solid waste (Christensen, 2011). The authors note that if the processed RDF needs to be stored for long periods of time before processing then an extra densification unit needs to be added within the facility that condenses the RDF into pellets (New York State Department of Environmental Conservation, 1990). The RDF facility has a significant capital cost associated with it. In a previous study, it represented around 25% of the total capital investment of an MSW facility (Jones et al., 2009).

2.1.2. Municipal solid waste gasification

The refuse derived fuel exiting the RDF facility is directed to the municipal solid waste gasification section, shown in Fig. 2. The representative composition of the RDF is shown in Table 1. The high moisture content associated with municipal solid waste is one of the main challenges associated with the processing of this feed. In this study, it is assumed that the moisture content of the RDF entering the gasification section is 28% (Krieth, 1994; Liu and Lipták, 1999; Choy et al., 2004). The RDF is first passed through a drier to reduce its moisture content to 8.80%. Flue gas generated within the refinery supplies the heat necessary for the drying step. The flue gas leaves the drier at 110 °C and 1.05 bar. Any particulates present within the flue gas are removed by passing the flue gas through an air cyclone and baghouse filter (National Renewable Energy Laboratory, 2011b). The flue gas is then vented to the atmosphere. The RDF exits the drier and is lockhopped into the MSW gasifier using compressed CO_2 (10 wt%).

The MSW gasifier operates at 30 bar, at either 800 °C, 850 °C, or 900 °C, and in the presence of a calcium dolomite catalyst. Either solid fuel or a combination of solid and vapor fuel are input into the gasifier. The decision at which temperature to operate at and what

Table 1
Feedstock proximate and ultimate analysis for a representative MSW sample (He et al., 2009).

Feed type	Proximate analysis (db, wt%)				Heating values (kJ/kg)	
	Moisture (ar)	Ash	VM[a]	FC[b]	HHV[c]	LHV[d]
RDF	28	5.93	82.28	11.79	N/A	21,306
Feed type	Ultimate analysis (db, wt%)					
	C	H	N	Cl	S	O
RDF	51.81	5.76	0.26	0	0.36	35.88

[a] Volatile matters.
[b] Fixed carbon.
[c] Higher heating value.
[d] Lower heating value.

type of fuel to input will be determined by the global optimization framework. The effluent exiting the MSW gasifier is a mixture of synthesis gas, C_1 and C_2 hydrocarbons, ash, tar, char, and acid gases such as NH_3 and H_2S. The effluent is passed through two MSW ash cyclones which separate the solid ash and char from the vapor phase products. Effectively 100% of the carbon present in the municipal solid waste is converted to vapor products by recycling the char back into the gasifier. The ash is ultimately output as slag.

The first paper (Onel et al., 2014) in this series described the parameter estimation optimization model that determined the optimal RDF gasifier parameters which minimized the error between experimental data and the model predicted effluent. The optimal parameters used for operation of the RDF gasifier are shown in Table 2. The effluent is a function of the MSW gasifier temperature, oxidizer flow rate, and MSW composition. Steam is input to gasify the fuel, while high-purity oxygen provides the heat necessary for the reforming reactions. The oxygen also facilitates the cracking of the tar species. Eqs. (1)–(18) govern the operation of the RDF gasifier. Before describing each equation, an explanation of the indices, sets, parameters, and variables present in the model is given.

The indices describing the MSW gasifier model include the following:

a : Atom index
s : Species index
x : Oxidizing input index

The set of all atoms is given by the following:

$$a \in A_{RDF} = \{\text{Ar, C, H, O, N, S}\}$$

The set of all species present in the gasifier is described by the following:

$$s \in S = \left\{ \begin{array}{l} \text{Ar, } C_{(s)}, CH_4, CO, COS, CO_2, C_2H_2, C_2H_4, C_2H_6, \\ \quad C_5H_8O_4, C_6H_{10}O_5, (C_2H_4)_n, (C_8H_8)_n, \\ C_6H_6, C_7H_8, mpC_8H_{10}, oC_8H_{10}, C_9H_{10}, C_9H_8, C_{10}H_8, \\ \quad 1\text{-}C_{11}H_{10}, \\ 2\text{-}C_{11}H_{10}, C_{12}H_8, a\text{-}C_{12}H_{10}, b\text{-}C_{12}H_{10}, f\text{-}C_{16}H_{10}, \\ \quad p\text{-}C_{16}H_{10}, C_6H_6O \\ C_{15}H_{14}O_4, C_{20}H_{22}O_{10}, C_{22}H_{28}O_9, HCN, H_2, H_2O, \\ \quad H_2S, NH_3, NO, N_2, N_2O, O_2 \end{array} \right\}$$

The set of all species present in the vapor phase is:

$$S_V = \left\{ \begin{array}{l} \text{Ar, } CH_4, CO, COS, CO_2, C_2H_2, C_2H_4, C_2H_6, \\ HCN, H_2, H_2O, H_2S, NH_3, NO, N_2, N_2O, O_2 \end{array} \right\}$$

The set of species, S_T, present in tar as a liquid phase is:

$$S_T = \left\{ \begin{array}{l} C_6H_6, C_7H_8, mpC_8H_{10}, oC_8H_{10}, C_9H_{10}, C_9H_8, C_{10}H_8, \\ \quad 1\text{-}C_{11}H_{10}, \\ 2\text{-}C_{11}H_{10}, C_{12}H_8, a\text{-}C_{12}H_{10}, b\text{-}C_{12}H_{10}, f\text{-}C_{16}H_{10}, \\ \quad p\text{-}C_{16}H_{10}, C_6H_6O \end{array} \right\}$$

A set of hydrocarbon species defined for convenience is:

$$S_{HC} = \{CH_4, C_2H_2, C_2H_4, C_2H_6\}$$

The RDF is composed of a set of species, S_{RDF}, which include hemicellulose, cellulose, lignin, and plastic monomers:

$$S_{RDF} = \{C_5H_8O_4, C_6H_{10}O_5, C_{15}H_{14}O_4, C_{20}H_{22}O_{10}, C_{22}H_{28}O_9, (C_2H_4)_n, (C_8H_8)_n\}$$

The set of all oxidizing feeds includes:

$$x \in Ox = \{\text{Oxygen, Air, Enriched Air}\}$$

The parameters used in the MSW gasifier model include the following:

$w_{moisture}$: fraction of water present in received RDF feedstock
w_{ash} : fraction of ash present in dry RDF feedstock
M_{RDF} : mass of RDF, dry ash-free (daf), per kg of RDF feedstock : $(1 - w_{moisture})(1 - w_{ash})$
UA_a : weight fraction of atom a present in daf RDF from normalized ultimate analysis
$w_{s,RDF}$: weight fraction of species s in daf RDF
$E_{a,s}$: number of atom a in species s
AW_a : atomic weight of atom a
MW_s : molecular weight of species s
M_a^{steam} : mass of atom a within RDF moisture per kg of daf RDF: $E_{a,H_2O} AW_a MW_{H_2O}^{-1} w_{moisture}$
M_x : mass flow rate of oxidizer x
$W_{s,x}$: percent weight of species s in oxidizer x
$g_s^o(T)$: Standard Gibbs' free energy of species s at temperature T
$\alpha_{s,s'}$: stoichiometric coefficient of product s' for the pyrolysis reaction of s

The variables in the gasifier model include the following:

$N_{C,a}$: molar atomic production of char during gasification
N_s : molar flow rate of species s
M_t : total mass flow rate of tar
$M_{t,n}$: tar mass fraction in the effluent
y_s : vapor mole fraction of species s

The MSW gasification model conserves the number of atoms, as well as the mass, for the overall gasifier, as shown in Eqs. (1) and (2):

$$\sum_{s' \in S} \alpha_{s,s'} E_{a,s} = E_{a,s}, \quad \forall s \in S_{RDF}, a \in A \tag{1}$$

$$M_{RDF} UA_a + M_a^{steam} + \sum_{s \in S_{Ox}} \sum_{x \in Ox} M_x W_{s,x} AW_a MW_s^{-1} E_{a,s} = N_{C,a} + \sum_s E_{a,s} N_s AW_a, \quad \forall a \in A \tag{2}$$

Additionally, char only contains carbon, so Eq. (3) is imposed:

$$N_{C,a} = 0, \quad a \in \{\text{Ar, H, O, N, S, Cl}\} \tag{3}$$

The temperature-dependent char formation equation (Eq. (4)) is shown below:

$$\sum_a N_{C,a} = (a_{Ch}^1 + a_{Ch}^2 T)(1 - w_{moisture}) \tag{4}$$

where a_{Ch}^1 and a_{Ch}^2 are parameters that were optimized.

The gasifier model assumes that the amount of tar formed is dependent on the operating temperature. The equations governing the tar formation are shown below (Eqs: (5)–(8)):

$$\sum_s (N_s \cdot MW_s) = M_t, \quad s \in S_T \tag{5}$$

$$M_{t,n} = \frac{M_t}{1 + M_x / M_{RDF}} \tag{6}$$

$$(N_s \cdot MW_s) = Fract_s \cdot M_t, \quad s \in S_T \tag{7}$$

$$M_t = (a_T^1 + a_T^2 T) \tag{8}$$

where a_T^1 and a_T^2 are parameters that were optimized.

Table 2
Optimized MSW gasifier model parameters.

Parameter	MSW
mf_N	0.900
fc_S	1.000
$fc^{HC}_{CH_4}$	2/3
$fc^{HC}_{C_2H_2}$	2/3
$fc^{HC}_{C_2H_4}$	2/3
$fc^{HC}_{C_2H_6}$	2/3
a^1_{Ch}	0.0001
a^2_{Ch}	-8.5×10^{-8}
a^1_T	0.001173
a^2_T	-1×10^{-6}
$a^1_{N_2}$	1.000005
$a^2_{N_2}$	-4.7×10^{-9}
$a^3_{N_2}$	-9×10^{-6}
$a^1_{NH_3}$	2.359×10^{-4}
$a^2_{NH_3}$	2.818×10^{-3}
a^1_{NO}	2.634×10^{-4}
a^2_{NO}	0.1111

It is assumed that complete combustion of the pyrolysis species takes place, so no oxygen is present in the vapor phase effluent. Additionally, since char is a solid, the following equation (Eq. (9)) is included to set restrictions on the species present in the vapor phase effluent of the gasifier:

$$N_s = 0, \quad s \in \{S_{RDF}, O_2, C_{(s)}\} \tag{9}$$

The molar composition of the vapor phase species can be calculated using Eq. (10):

$$N_s = y_s \sum_s N_s, \quad \forall s \in S_V \tag{10}$$

It is assumed that the water-gas-shift reaction is in thermodynamic equilibrium in the vapor phase effluent, therefore Eq. (11) is imposed:

$$\frac{y_{CO_2}\cdot y_{H_2}}{y_{H_2O}\cdot y_{CO}} = \exp\left(\frac{g^o_{CO_2} + g^o_{H_2} - g^o_{H_2O} - g^o_{CO}}{RT}\right) \tag{11}$$

The values for g^o_s may be explicitly determined from the NASA polynomials, as shown in Eq. (12):

$$\frac{g^o_s}{RT} = -\frac{A_1T^{-2}}{2} + \frac{2A_2(1-\ln(T))}{T} + A_3(1-\ln(T)) - \frac{A_4T}{2} - \frac{A_5T^2}{6} - \frac{A_6T^3}{12} - \frac{A_7T^4}{20} + \frac{A_8}{T} - A_9 \tag{12}$$

The hydrocarbon species present in the gasifier effluent are not in thermodynamic equilibrium, and therefore the molar flow rates are determined using Eq. (13):

$$fc^{HC}_s \sum_{s'\in S_{RDF}} w_{s',MSW} MW^{-1}_{s'} \alpha_{s',s} = N_s, \quad \forall s \in S_{HC} \tag{13}$$

where fc^{HC}_s are parameters that were optimized.

The total molar fraction of N present as either N_2 or NH_3 is mf_N, a parameter that was optimized. Eq. (14) governs this relationship:

$$mf_N \cdot M_{RDF} \cdot UA_N + \sum_{x\in Ox} M_x \cdot W_{N_2,x} = N_{N_2}\cdot MW_{N_2} + N_{NH_3}\cdot MW_{NH_3} \tag{14}$$

The relative proportion of N_2 and NH_3 is a linear function of system temperature (Zhou, 1997) and the corresponding equation governing this relationship (Eq. (15)) is shown below:

$$N_{N_2} = \left[a^1_{N_2} + a^2_{N_2}\cdot(T + a^3_{N_2})\right]\left(N_{N_2} + N_{NH_3}\right) \tag{15}$$

where $a^1_{N_2}$, $a^2_{N_2}$, and $a^3_{N_2}$ are parameters that were optimized.

Also, the relative ratio of HCN to NH_3 is a function of the H/N content of the fuel. The relative ratio of N_2O to NO is a function of the O/N content of the fuel. These relationships are described in the following equations (Eqs. (16) and (17)):

$$N_{NH_3} = \left(a^1_{NH_3}\cdot\frac{UA_HAW_N}{UA_NAW_H} + a^2_{NH_3}\right)\cdot N_{HCN} \tag{16}$$

$$N_{NO} = \left(a^1_{NO}\cdot\frac{UA_OAW_N}{UA_NAW_O} + a^2_{NO}\right)\cdot N_{N_2O} \tag{17}$$

where $a^1_{NH_3} = 2.359E-4$, $a^2_{NH_3} = 2.818E-4$, $a^1_{NO} = 2.634E-4$, and $a^2_{NO} = 0.1111$. These values were previously determined by Baliban et al. (2010) by using experimental data presented in Table 4 of Stubenberger et al. (2008).

The decomposition of sulfur is distributed between H_2S and COS and is represented in Eq. (18):

$$fc_S \cdot M_{RDF}\cdot UA_S = N_{H_2S}\cdot AW_S \tag{18}$$

where fc_S is a parameter that was optimized.

Although a calcium dolomite catalyst is utilized to reform the tar in the gasifier, the effluent of the gasifier is passed through a catalytic tar reformer that operates at 925 °C. The National Renewable Energy Laboratory provides a bench-scale performance of a tar cracker, which is also being installed for pilot-plant scale demonstration (National Renewable Energy Laboratory, 2011b,a). The reformer converts 99.6% of tars, 99% of C_2H_6, 90% of C_2H_4, 90% of NH_3, and 80% of CH_4 (National Renewable Energy Laboratory, 2011b). No additional steam is required as input into the tar cracker (National Renewable Energy Laboratory, 2011a), whereas heat for the endothermic reforming reactions are supplied by the circulating and regenerating catalyst, as well as additional combustion gases that are passed through the regeneration system (National Renewable Energy Laboratory, 2011a). The cost of all ash cyclones, as well as the cost of the catalytic tar reformer, is included in the cost of the municipal solid waste gasifier, shown in Table 3. The ash cyclones and the catalytic tar reformer are included in the process synthesis superstructure to prevent contamination of the downstream hydrocarbon production and upgrading reactors. The effluent from the tar cracker is sent to the syngas cleaning section.

2.2. Synthesis gas cleaning

The municipal solid waste syngas exiting the tar cracker is sent to the syngas cleaning section, shown in Fig. 3. The syngas can either be sent to a dedicated sour water-gas-shift (WGS) reactor or can bypass the WGS reactor, where it is cooled to 185 °C and is directed to the scrubbing system. The dedicated WGS reactor operates in the presence of sulfur species, at a pressure of 26 bar, between 300 and 600 °C, and can facilitate either the forward or reverse WGS reaction. The forward WGS reaction increases the H_2/CO syngas ratio, but at the expense of producing additional CO_2. The additional CO_2 generated will be removed in subsequent treatment units. Steam will be generated to handle the exothermicity of the forward WGS reaction. The reverse water-gas-shift reaction decreases the CO_2 concentration in the syngas. In order to be implemented effectively, the reverse WGS reaction generally requires a high inlet concentration (> 0.5) of CO_2 that can be achieved by recycling CO_2 from the process. Additional H_2 generated by the pressure swing adsorption (PSA) unit, electrolyzer, or autothermal reactor will facilitate the reverse WGS reaction. The heat necessary for the reverse WGS

Table 3
WTL refinery upgrading unit reference capacities, costs (2014 $), and scaling factors.

Description	C_o (MM$)	S_o	S_{Max}	Units	Scale basis	*sf*	Ref.
MSW gasification							
MSW handling & RDF facility	$ 94.82	45.2	33.3	kg/s	As received MSW	0.77	a
MSW gasification	$ 54.11	17.9	33.3	kg/s	Dry MSW	0.7	b
Synthesis gas handling/clean-up							
Water-gas-shift unit	$ 3.67	150	250	kg/s	Feed	0.67	d
Rectisol unit	$ 31.46	2.51	8.78	kmol/s	Feed	0.63	c
Hydrocarbon production							
Fischer–Tropsch unit	$ 12.01	23.79	60	kg/s	Feed	0.72	e,f
Hydrocarbon recovery column	$ 0.64	1.82	25.2	kg/s	Feed	0.7	g
Methanol synthesis	$ 8.06	35.647	–	kg/s	Feed	0.65	d
Methanol degasser	$ 3.74	11.169	–	kg/s	Feed	0.7	d
Methanol-to-gasoline unit	$ 5.68	10.6	–	kg/s	Feed	0.65	h,d
Methanol-to-olefins unit	$ 3.41	10.6	–	kg/s	Feed	0.65	h
Hydrocarbon upgrading							
Distillate hydrotreater	$ 2.21	0.36	81.9	kg/s	Feed	0.6	g
Kerosene hydrotreater	$ 2.21	0.36	81.9	kg/s	Feed	0.6	g
Naphtha hydrotreater	$ 0.67	0.26	81.9	kg/s	Feed	0.65	g
Wax hydrocracker	$ 8.25	1.13	72.45	kg/s	Feed	0.55	g
Naphtha reformer	$ 4.60	0.43	94.5	kg/s	Feed	0.6	g
C_5–C_6 isomerizer	$ 0.84	0.15	31.5	kg/s	Feed	0.62	g
C_4 isomerizer	$ 9.30	6.21	–	kg/s	Feed	0.6	g
C_3–C_5 alkylation unit	$ 51.23	12.64	–	kg/s	Feed	0.6	g
Saturated gas plant	$ 7.67	4.23	–	kg/s	Feed	0.6	g
FT ZSM-5 reactor	$ 4.83	10.6	–	kg/s	Feed	0.65	e,f
Olefins-to-gasoline/diesel unit	$ 3.41	10.6	–	kg/s	Feed	0.65	h
CO_2 separation unit	$ 5.28	8.54	–	kg/s	Feed	0.62	h
Deethanizer	$ 0.57	5.13	–	kg/s	Feed	0.68	h,d
Absorber column	$ 0.89	0.96	–	kg/s	Feed	0.68	h,d
Stabilizer column	$ 1.01	4.57	–	kg/s	Feed	0.68	h,d
Splitter column	$ 0.99	3.96	–	kg/s	Feed	0.68	h,d
HF alkylation unit	$ 8.80	0.61	–	kg/s	Feed	0.65	h,d
LPG/alkylate splitter	$ 1.04	0.61	–	kg/s	Feed	0.68	h,d
Hydrogen/oxygen production							
Pressure-swing absorption	$ 7.80	0.29	–	kmol/s	Purge gas	0.65	b
Air separation unit	$ 27.05	21.3	41.7	kg/s	O_2	0.5	b
Air compressor	$ 5.91	10	30	MW	electricity	0.67	b
Oxygen compressor	$ 7.91	10	20	MW	Electricity	0.67	b
Electrolyzer	$ 489.89	1	–	kW	Electricity	0.9	b
Light gas recycle							
Auto-thermal reformer	$ 10.69	12.2	35	kg/s	Natural gas feed	0.67	g
Heat and power integration							
Gas turbine	$ 79.94	266	334	MW	Electricity	0.75	b
Steam turbine	$ 64.95	136	500	MW	Electricity	0.67	b
Wastewater treatment							
Sour stripper	$ 3.92	11.52	–	kg/s	Feed	0.53	i
Biological digestor	$ 4.65	115.74	–	kg/s	Feed	0.71	j
Reverse osmosis	$ 0.31	4.63	–	kg/s	Feed	0.85	j
Cooling tower	$ 3.97	4530.3	–	kg/s	Feed	0.78	i

a. Jones et al. (2009); b. Larson et al. (2009a); c. Kreutz et al. (2008); d. National Renewable Energy Laboratory (2011b); e. Mobil Research and Development Corporation (1983); f. Mobil Research and Development Corporation (1985); g. Bechtel Corporation (1998); h. Mobil Research and Development Corporation (1978); i. National Energy Technology Laboratory (2007); j. Balmer and Mattsson (1994).

reaction will be provided by combustion of the syngas species via oxygen produced from the air separation unit or electrolyzer. The decision to include the dedicated WGS reactor depends on: (i) the $H_2/(CO+CO_2)$ ratio needed for syngas conversion, (ii) the amount of H_2 that can economically be removed using the PSA unit, (iii) the economics associated with H_2 production using an electrolyzer, and (iv) the lifecycle greenhouse gas emissions constraint for the WTL refinery. If the dedicated WGS reactor is selected, the effluent is cooled to 185 °C and mixed with any bypass raw syngas before being sent to the scrubbing system.

Any residual tar, particulates, and NH_3 within the raw syngas are removed in the sour syngas scrubber. The effluent is directed to a dual-capture methanol absorption system (Rectisol unit) that co-removes 100% of the H_2S and 90% of the CO_2 from the syngas. No pollutants are present downstream of the synthesis gas cleaning section so that they do not affect downstream reactor performance. The H_2S and CO_2 are captured in separate streams and the molar ratio of CO_2 to H_2S in the sulfur-rich stream is 3:1 (Kreutz et al., 2008). The Rectisol system is a necessary component of the WTL refinery because it protects the methanol synthesis and Fischer–Tropsch reactors from catalyst poisoning. The Claus recovery system inputs the sulfur-rich stream from the Rectisol unit and converts the 95% of the H_2S and SO_2 into solid sulfur (National Energy Technology Laboratory, 2007). In order to recover 100% of the sulfur from the WTL refinery, the tail gas from the Claus recovery system is hydrogenated to H_2S and recycled back to the Recistol unit. The carbon dioxide recovered from the acid gas recovery units may be utilized in one of the following three ways: (i) compressed to 31 bar and recycled in the WTL refinery, (ii) compressed to 150 bar for sequestration, or (iii) vented from the WTL plant.

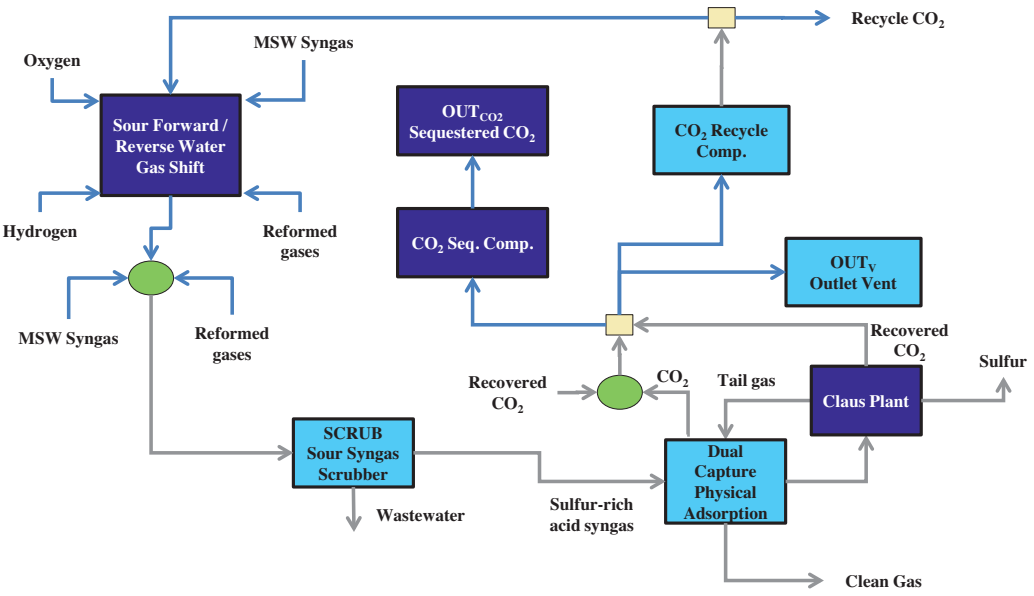

Fig. 3. Synthesis gas cleaning flowsheet. Syngas is either sent to a dedicated forward/reverse WGS reactor or bypasses this unit and is sent to the scrubbing system. The effluent from the scrubber is directed to a Rectisol unit which removes the H_2S and CO_2 in the raw syngas. A Claus plant recovers solid sulfur from the H_2S gas. CO_2 recovered in the process can either be recycled in the WTL refinery, sequestered, or vented to the atmosphere.

The first two options utilize inter-stage cooling that ensures the temperature from the compressor outlet does not exceed 200 °C.

2.3. Hydrocarbon production & upgrading

2.3.1. Fischer–Tropsch hydrocarbon production

Fig. 4 shows one possible conversion option for the MSW syngas exiting the cleaning section. The clean syngas may be split to any one of six possible Fischer–Tropsch (FT) reactors. Two of the FT reactors considered use cobalt-based catalysts, while the other four utilize iron-based catalysts. Each of the FT reactors operates at 20 bar and will be discussed in this section.

The main difference between the Co- and Fe-based FT reactors is their ability to promote WGS activity. Fe-based FT reactors can catalyze the WGS reaction and consume any CO_2 produced in the refinery by mixing it with H_2-rich syngas or inputting H_2 gas produced in the WTL refinery (Baliban et al., 2011, 2012b,c). In order for CO_2 to be consumed via the reverse WGS reaction, the ratio of $CO_2/(CO+CO_2)$ needs to be above a critical threshold that depends on the relative amount of H_2 with respect to CO and CO_2 (Baliban et al., 2013e,a). If the ratio of $CO_2/(CO+CO_2)$ is below the critical threshold, CO will be converted to CO_2 via the forward WGS reaction. Low temperature Fe-based units have been successfully operated using inlet H_2/CO ratios between 0.5 and 1.0 and produced effluents with an H_2/CO ratio between 1.7 and 2.0. Despite using less H_2 than units that input H_2/CO ratios near 2, as much as half of the CO was converted to CO_2. The outlet concentration of CO_2 can be controlled by setting the $H_2/(CO+CO_2)$ ratio so that CO_2 is used as a carbon source. The $H_2/(2CO+3CO_2)$ ratio is defined as the Ribblett ratio (de Klerk, 2011; Steynberg and Dry, 2004) when it is approximately equal to 1 and is highly beneficial because the inlet syngas and unreacted syngas in the effluent have the same composition. Thus, high conversion rates of CO and CO_2 can be achieved by designing internal and external gas loops.

The effects of the $H_2/(CO+CO_2)$ ratio will be investigated in the following two ways. Two FT reactors (LTFTRGS – 240 °C and HTFTRGS – 320 °C) will require an inlet Ribblett ratio of 1. These two units will facilitate the reverse WGS reaction. The other two Fe-based (medium-temperature nominal wax FT, MTFTWGS-N, and medium-temperature minimal wax FT, MTFTWGS-M) units will require an inlet H_2/CO ratio between 0.5 and 0.7 and operate at a temperature of 267 °C. The effluent H_2/CO ratio in these units will be approximately 1.7 through the forward WGS reaction. These two units are modeled after the ones presented by Mobil Research & Development (Baliban et al., 2012c; Mobil Research and Development Corporation, 1983, 1985). Additionally, the H_2/CO ratio within these FT units can also be shifted by inputting steam.

Two types of Co-based FT units will be examined in this paper: high-temperature (HTFT – 320 °C) and low-temperature (LTFT – 240 °C) reactors. Since the Co-based FT units do not promote WGS activity (de Klerk, 2011), high per-pass conversion of CO to FT liquids can be achieved. However, product selectivity can change due to the deactivation of the cobalt catalyst. Deactivation has been attributed to carbon disposition and fouling, oxidation and mixed-oxide formation, and changes in cobalt crystallite size (de Klerk, 2011). Carbon disposition and fouling generally form a physical barrier or change the chemical nature of the catalyst (de Klerk, 2011). However, deactivation that occurs because of preventation to catalytic sites can be reversed by removing the carbonaceous deposits by rejuvenating or regenerating the catalyst (de Klerk, 2011). Deactivation due to oxidation is a contentious topic because of conflicting reports of the causes responsible for loss of cobalt catalyst activity. Therefore, this study sets the CO per-pass conversion to 60% to prevent catalyst oxidation. The authors note that if catalyst stability can be achieved, conversions up to 80% can be achieved. The high-temperature cobalt-based FT reactor has not been commercially available yet, but a typical alpha value of 0.72 that is often associated with high-temperature FT operation is used to model the Co-based HTFT reactor.

Any one of the six FT reactors described can input additional hydrogen to shift the H_2/CO or H_2/CO_2 ratios. The vapor phase effluent exiting the FT units is directed to the upgrading section (described in the next section), while any wax generated is sent to the wax hydrocracker.

2.3.2. Fischer–Tropsch hydrocarbon upgrading

The process synthesis superstructure includes two alternatives for upgrading the hydrocarbon effluent leaving the FT reactors. The first option includes passing it through a ZSM-5 catalytic reactor operating at 408 °C and 16 bar which upgrades the FT effluent

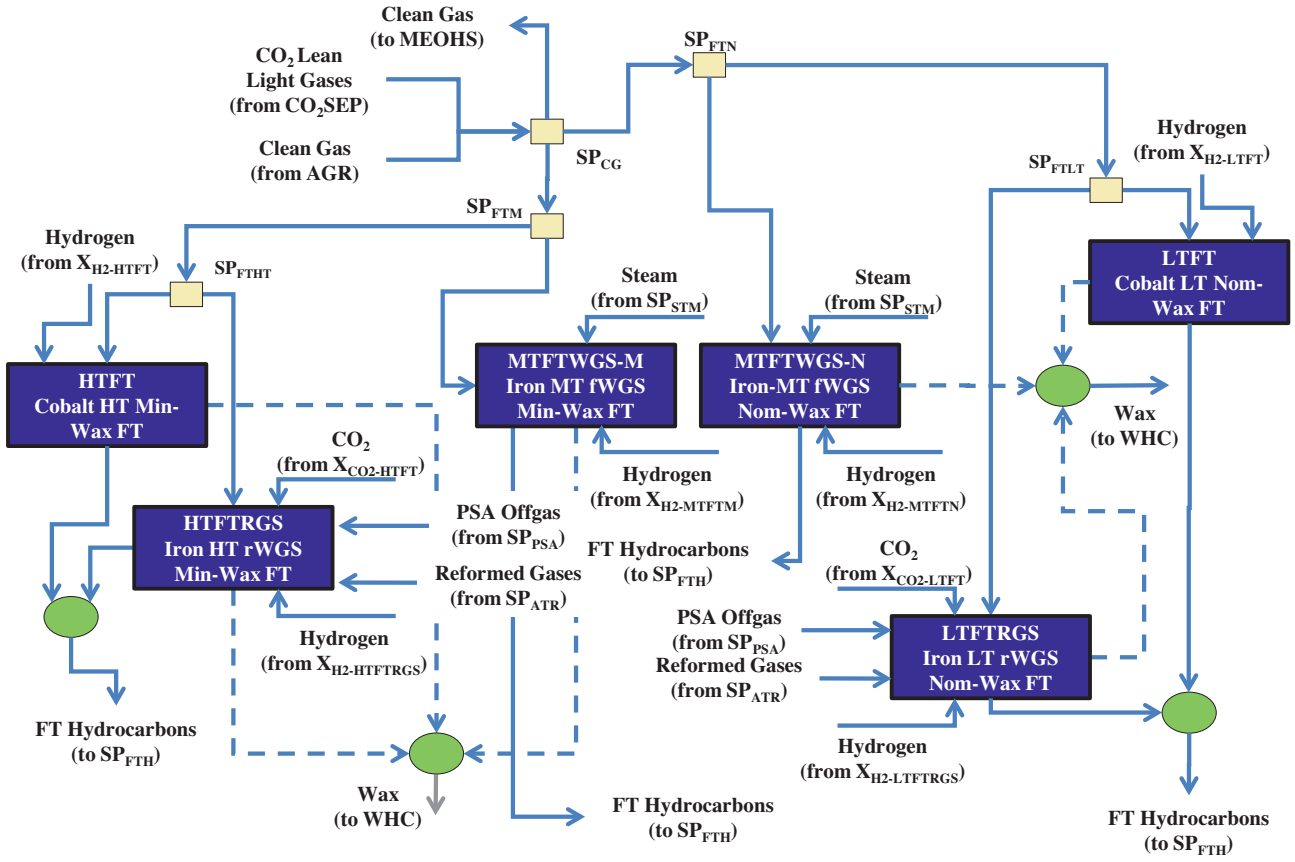

Fig. 4. Fischer–Tropsch hydrocarbon production flow diagram. Clean syngas may be split within six Fischer–Tropsch reactors operating with either an iron-based or cobalt-based catalyst.

into gasoline range hydrocarbons and some distillate, as shown in Fig. 5 (Mobil Research and Development Corporation, 1983, 1985). The ZSM-5 catalytic reactor will be able to convert the oxygenates within the FT effluent into additional hydrocarbons. The water, distillate, and gasoline product present in the effluent of the ZSM-5 catalytic reactor are separated in a fractionation unit and sent to the wastewater treatment section, distillate hydrotreater, and LPG-gasoline separation section, respectively. The ZSM-5 reactor effluent is modeled after one presented by Mobil (Mobil Research and Development Corporation, 1983, 1985).

Alternatively, the vapor phase effluent may be directed to a series of treatment units that cool and scrub the stream and remove the aqueous phase and any oxygenates present, also shown in Fig. 5. The extracted water and oxygenates are directed to the wastewater treatment section. The water lean FT hydrocarbons are then separated into C_3–C_5 gases, naphtha, kerosene, distillate, wax, offgas, and wastewater in a hydrocarbon recovery system, illustrated in Fig. 6 (Bechtel Corporation, 1998; Baliban et al., 2010). The individual streams exiting the hydrocarbon recovery column are upgraded in a series of units which include a wax hydrocracker, a distillate hydrotreater, a kerosene hydrotreater, a naphtha hydrotreater, a naphtha reformer, a C_4 isomerizer, a C_5/C_6 isomerizer, a $C_3/C_4/C_5$ alkylation unit, and a saturated gas plant (Bechtel Corporation, 1998, 1992). The operation of these units and the upgrading of each stream has been described in previous works (Baliban et al., 2010, 2012c).

2.3.3. Methanol synthesis

The sulfur-free synthesis gas exiting the syngas cleaning section is compressed to 51 bar before entering the methanol synthesis reactor operating at 300 °C and 50 bar, shown in Fig. 7. The water-gas-shift reaction (Eq. (19)) and the methanol synthesis reaction (Eq. (20)) are assumed to exist within equilibrium in the reactor (National Renewable Energy Laboratory, 2011b):

$$CO + H_2O \leftrightarrow CO_2 + H_2 \quad (19)$$

$$CO + 2 \cdot H_2 \leftrightarrow CH_3OH \quad (20)$$

The amount of CO_2 in the synthesis gas entering the methanol synthesis reactor will have important consequences on the composition of the effluent exiting this unit. If the CO_2 concentration in the input increases, additional water will be generated through the reverse WGS reaction and the per-pass conversion of carbon monoxide and carbon dioxide would decrease. However, if the input stream has a Ribblett ratio of 1, then the CO and CO_2 can be recycled back to the reactor, resulting in an overall conversion of CO and CO_2 greater than 90%. Downstream purification of the methanol is not considered because the methanol conversion units are tolerant to higher concentrations of water in the output and can handle as much as 50 wt% water. Since the methanol conversion units will produce around 50 wt% water from hydrocarbon synthesis, high concentrations of water within the methanol input are not assumed to be a concern (Tabak and Yurchak, 1990).

The raw methanol effluent exiting the synthesis reactor is cooled to 35 °C and flashed to separate the entrained vapor from the methanol product. 95% of the vapor phase is recycled back to the methanol synthesis reactor and the balance is used as fuel gas in the process. A majority (95%) of the crude methanol product entering the flash unit is recovered and heated to 300 °C to form a gas that is expanded to 5 bar in a turbine to recover electricity. The

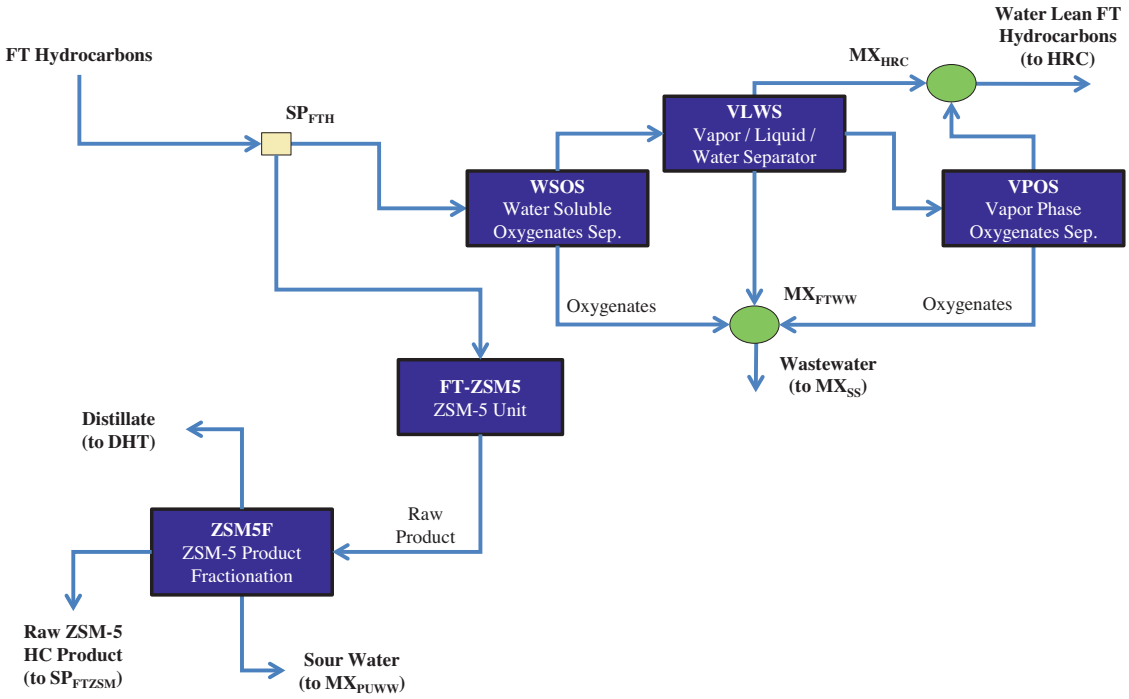

Fig. 5. Fischer–Tropsch hydrocarbon upgrading flow diagram. The FT hydrocarbons may be sent to either a ZSM-5 catalytic reactor or to a series of treatment units that knock out the water/oxygenates present in the stream.

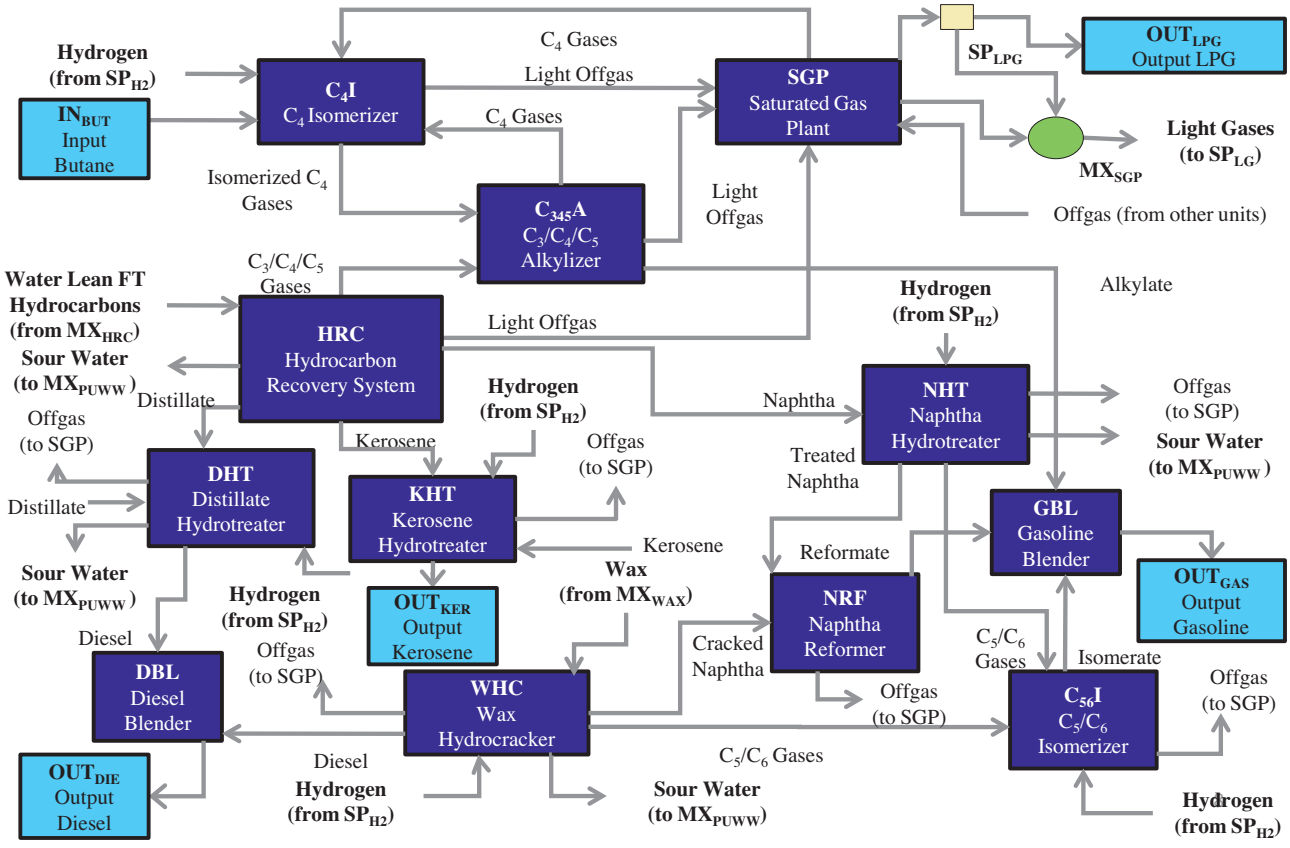

Fig. 6. Fischer–Tropsch hydrocarbon upgrading flow diagram. The water-lean FT hydrocarbons are directed to a series of upgrading units that separate the naphtha and distillate.

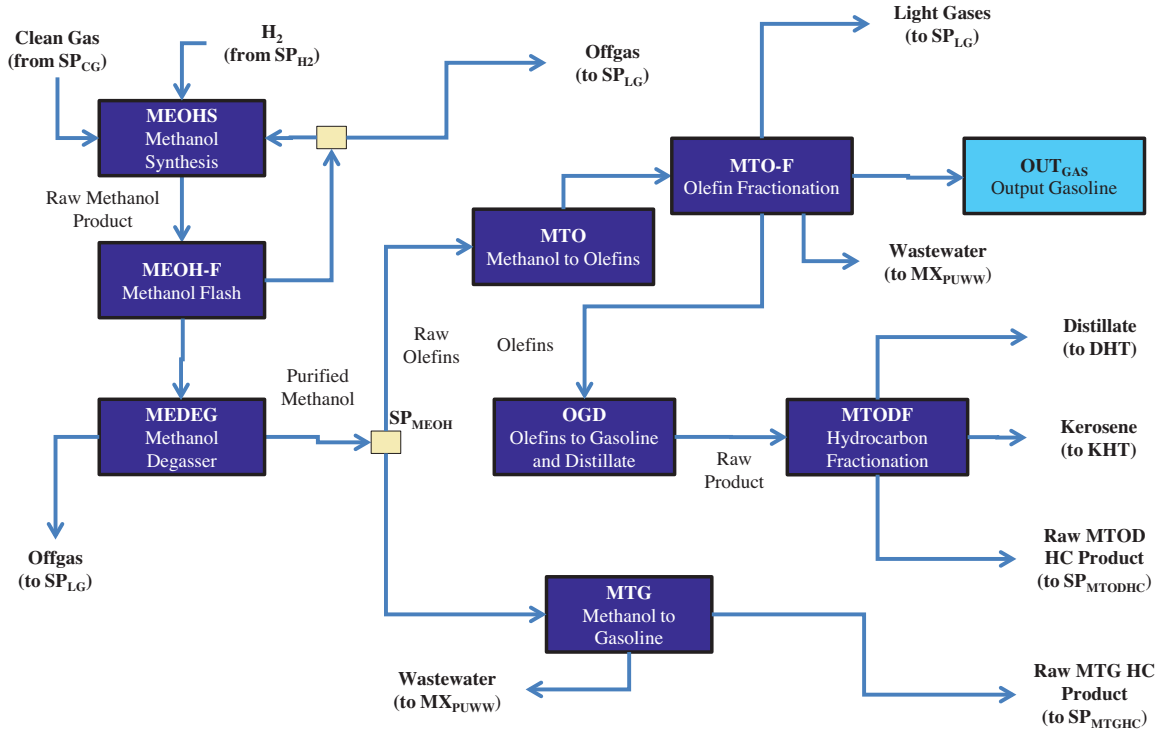

Fig. 7. Methanol synthesis and conversion flow diagram. Syngas is converted to methanol which is then sent to either the methanol-to-gasoline reactor or to the methanol-to-olefins reactor. The olefins are directed to the Mobil olefins-to-gasoline/distillate technology.

turbine effluent is directed to a degasser distillation column after being cooled to 60 °C. The degasser removes the entrained gases and recovers 99.9 wt% of the methanol. The gases will be recycled as fuel gas within the WTL refinery, and the bottoms product, which is a mixture of methanol and water, is split to one of two methanol conversion reactors.

2.3.4. Methanol conversion

The process synthesis superstructure currently contains two alternatives for methanol conversion, both of which will be described in this section and are shown in Fig. 7. The methanol-to-gasoline (MTG) adiabatic reactor operates at 400 °C and 12.8 bar. Prior to entering the fluidized bed reactor, the methanol is pre-heated to 330 °C and its pressure is raised to 14.5 bar. A ZSM-5 catalyst converts the methanol into gasoline-range hydrocarbons. Table 3.4.2 of a Mobil study (Mobil Research and Development Corporation, 1978) and Process Flow Diagram P850-A1402 of a National Renewable Energy Laboratory (NREL) study (National Renewable Energy Laboratory, 2011b) outline the MTG effluent. The MTG reactor is modeled using an atomic balance that represents the one presented in the NREL study. The methanol will be converted to 56 wt% water and 44 wt% hydrocarbons (National Renewable Energy Laboratory, 2011b; Mobil Research and Development Corporation, 1978). The hydrocarbons are decomposed as follows: 2 wt% are light gases, 19 wt% are C_3–C_4 gases, and 79 wt% is the gasoline product. The gasoline product is upgraded in the LPG–gasoline separation section, described later in the text, and the final products contain 82 wt% gasoline, 10 wt% LPG, and 8 wt% recycle gases (National Renewable Energy Laboratory, 2011b).

Alternatively, the methanol can be heated to 400 °C at 1.2 bar and can be directed to the methanol-to-olefins (MTO) reactor that operates at 375 °C and 1 bar (Mokrani and Scurrell, 2009; Tabak and Yurchak, 1990). A SAPO-34 catalyst converts 100% of the methanol and the input carbon is converted into over 93 wt% C_2–C_4 olefins (Mokrani and Scurrell, 2009). The effluent from the MTO reactor is fractionated and all of the olefins generated are sent to the Mobil olefins-to-gasoline-and-distillate (MOGD) process, all of the C_1–C_3 alkanes are recycled back to the refinery, all of the C_5 species are blended into the gasoline pool, and all of the water is sent to the wastewater treatment section.

The MOGD unit operates at 400 °C and 1 bar and uses a ZSM-5 catalyst to convert the olefins into gasoline and distillate (Tabak et al., 1986; Tabak and Yurchak, 1990). Depending on the desired products output, the MOGD reactor can either operate in maximum distillate or maximum gasoline mode. At constant pressure and temperature, different olefinic feeds do not have a large effect on the production distribution (Tabak et al., 1986). The MOGD unit is modeled using an atomic balance and the ratio of gasoline to distillate is allowed to range between 0.12 and >100 (Tabak and Yurchak, 1990). The exothermic heat of reaction will be controlled by the generation of low pressure steam. The diesel, kerosene, gasoline, and light gases from the MOGD effluent will be separated through fractionation. The model assumes that all of the C_{11}–C_{13} species are separated as kerosene and the C_{14+} species are separated as diesel.

2.3.5. LPG–gasoline separation

The ZSM-5 catalytic conversion of the FT hydrocarbons and the MTG and MTO/MOGD reactors generate a mixture of LPG and gasoline that must be separated. The process flow sheet for this separation is shown in Fig. 8. Light gases are knocked out from the hydrocarbon mixture and the crude hydrocarbon liquid is directed to a de-ethanizer column. The de-ethanizer separates the C_1–C_2 hydrocarbons from the gasoline mixture. These light gases are sent to an absorber column that strips any leftover C_3+ species by using lean oil as the absorbing liquid (National Renewable Energy Laboratory, 2011b). The light gases are recycled back to the WTL

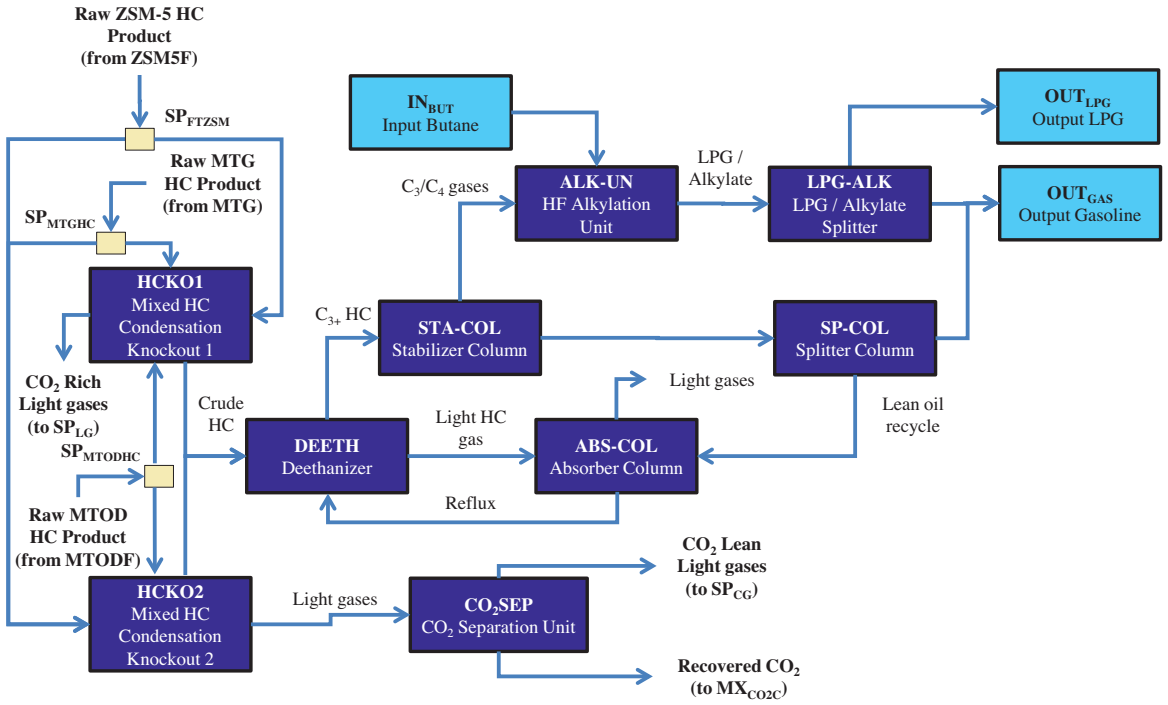

Fig. 8. LPG–gasoline separation flowsheet. The hydrocarbon product from the ZSM-5 catalytic conversion of the FT hydrocarbons or the methanol conversion units is sent to a series of treatment units that separate the gasoline from the LPG byproduct.

refinery, while the bottoms are refluxed to the de-ethanizer. The de-ethanizer bottoms are directed to the stabilizer column which separates the butanes from the gasoline range hydrocarbons. The gasoline is directed to a splitter column that sends a portion of the inlet to the absorber column to be used as the absorbing liquid, while the balance is sent to the gasoline pool. The butanes extracted from the stabilizer column are alkylated to produce isooctane and LPG (National Renewable Energy Laboratory, 2011b). The low pressure steam and cooling water required for this section was derived from an NREL study (National Renewable Energy Laboratory, 2011b).

2.4. Light gas handling

The light gases (C_1–C_2 hydrocarbons, unreacted syngas, and inert species) generated within the WTL refinery will be handled in one of two ways. An internal gas loop configuration can be designed that recycles the light gases exiting the Fischer–Tropsch and methanol synthesis reactors back to these units. These light gases may contain large amounts of unreacted H_2 and CO which can increase the overall conversion to liquid fuels if they are recycled back to the hydrocarbon production reactors. A portion of the recycled light gases in the internal gas loop configuration must be purged to prevent the build-up of inert species. The purged gases are directed to the external gas loop configuration.

The external gas loop configuration handles any light gases that are purged or not utilized in the internal gas loop configuration. Three options exist for the light gases in the external gas loop configuration, as shown in Fig. 9. A gas turbine will expand the light gases and produce electricity for the WTL refinery. The fuel combustor will provide process heat for any units in the WTL refinery. An autothermal reactor can reform the light gases into syngas that can be recycled back to the hydrocarbon production section. The fuel combustor and gas turbine effluents are cooled to 35 °C and sent to a knock-out unit that separates out the water. The effluent from the knock-out unit can either be vented to the atmosphere or passed through a CO_2 recovery unit.

2.5. Hydrogen/oxygen production

The hydrogen and oxygen requirements for the WTL refinery will be handled as follows. A pressure-swing adsorber can supply the necessary hydrogen, while an air separation unit can supply the oxygen needed in the refinery. Alternatively, if neither of these options are selected, an electrolyzer has the capability of providing both of these utilities. The process flow diagram for the hydrogen and oxygen production section is shown in Fig. 10.

2.6. Wastewater treatment

The complete process and utility wastewater treatment sections are outlined in Figs. 11 and 12, respectively. A biological digestor and a sour stripper will be utilized to remove the H_2S, NH_3, and oxygenates in the wastewater streams. The Claus combustor will input the sulfur-rich streams from the biological digestor and sour stripper and recover the sulfur. The Claus combustor will also provide heat for steam production. The wastewater network will send steam to process units in the WTL refinery, provide the process water that is necessary for electrolysis, and output wastewater from the WTL refinery (Baliban et al., 2012b).

2.7. Unit costs

Eq. (21) explicitly illustrates the calculation of the total direct cost, TDC, of each unit in the WTL refinery:

$$TDC = (1 + BOP) \cdot C_o \cdot \left(\frac{S_r}{S_o}\right)^{sf} \quad (21)$$

and uses the base component cost, C_o, the base component size (capacity), S_o, the actual component size (capacity), S_r, the scaling cost factor, sf, and the balance of plant, BOP, percentage. The

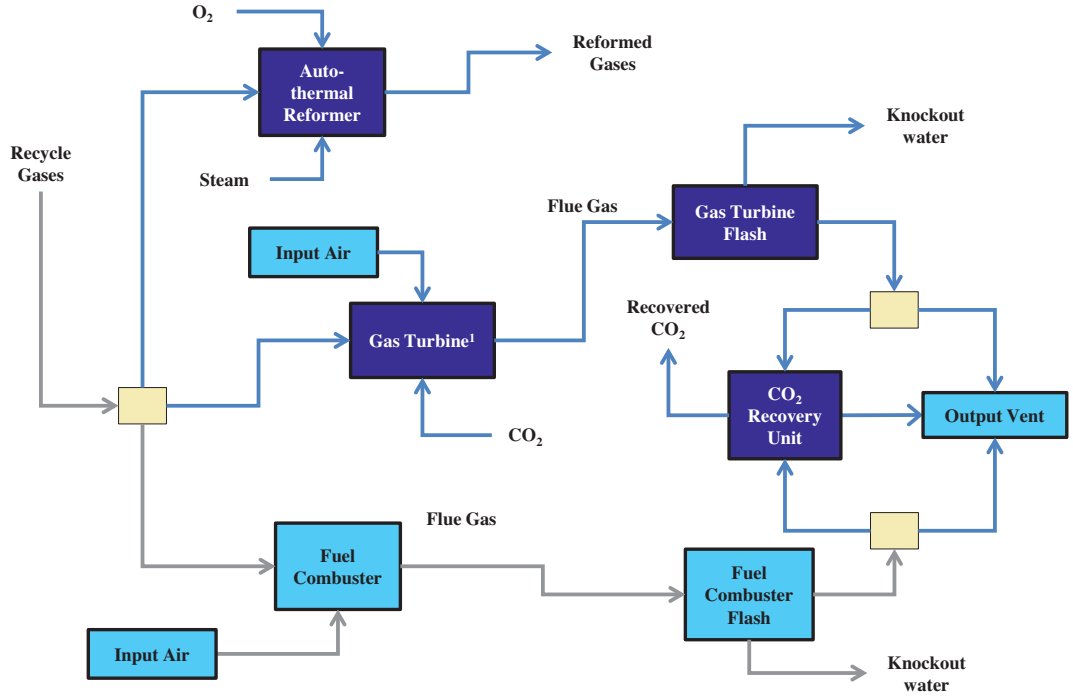

Fig. 9. Light gas handling flowsheet. Light gases produced in the WTL refinery can be directed to either the autothermal reformer, gas turbine, or fuel combustor.

balance of plant percentage (site preparation, civil works, utility plants, etc.) is assumed to be 20% of the total installed cost. Several literature sources are used to estimate the cost parameters used in Eq. (21) and are shown in Table 3 (Larson et al., 2009a; Kreutz et al., 2005; Kreutz et al., 2008; National Renewable Energy Laboratory, 2011b; National Energy Technology Laboratory, 2007; Mobil Research and Development Corporation, 1983, 1985, 1978; Bechtel Corporation, 1998; Balmer and Mattsson, 1994; Gregor et al., 1989;

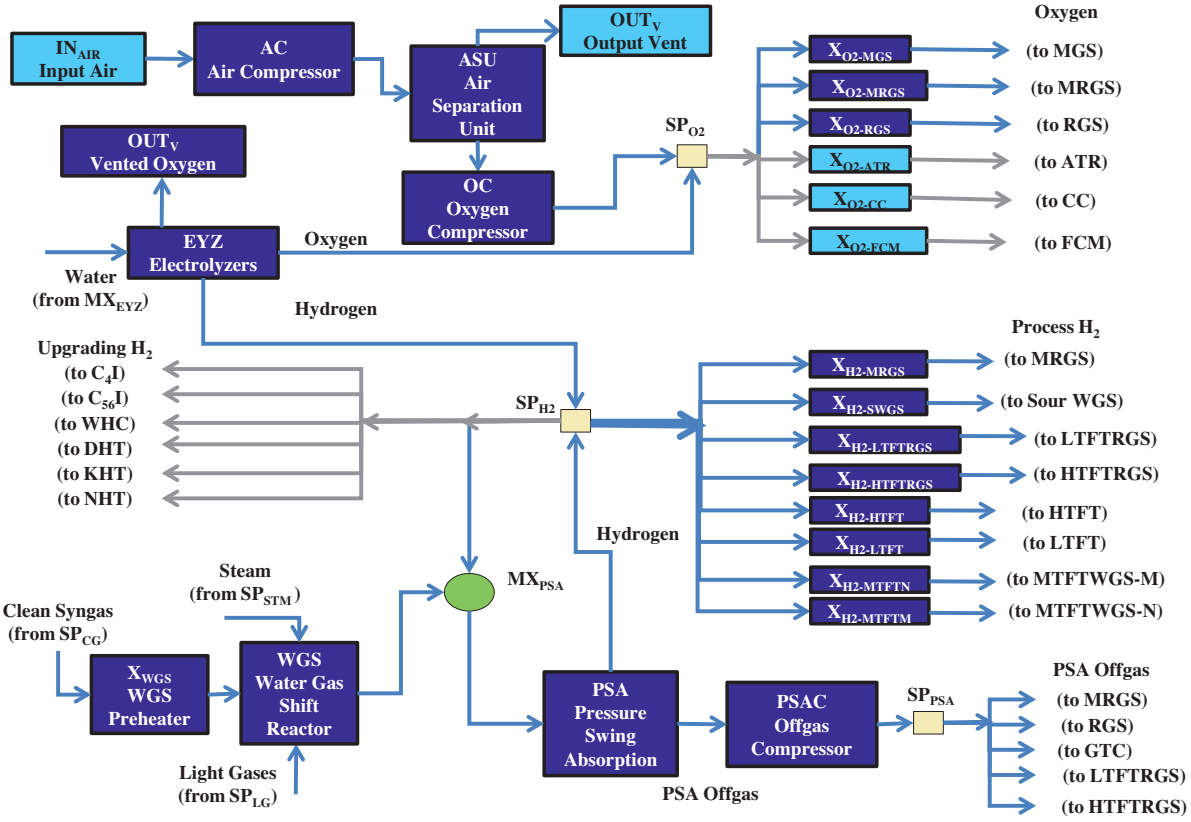

Fig. 10. Hydrogen & oxygen production section. Hydrogen in the WTL refinery is supplied through either the PSA or electrolyzer, while oxygen is produced from the electrolyzer or air separation unit.

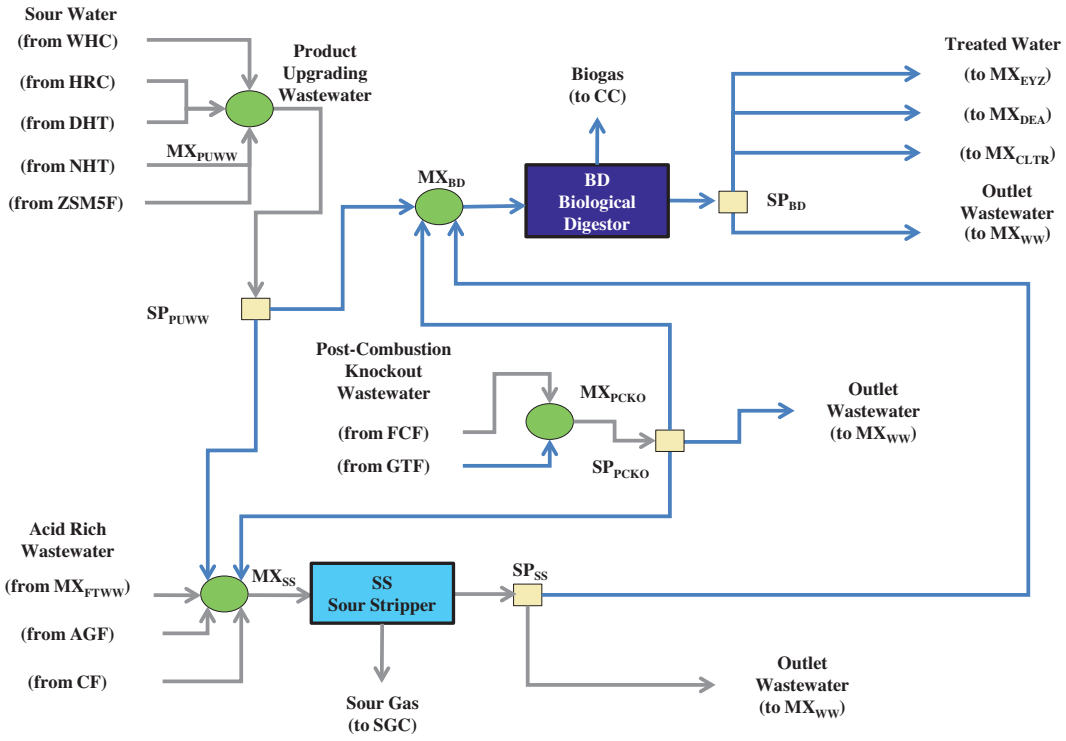

Fig. 11. Process wastewater treatment section.

Meyers, 2003; Jones et al., 2009). All costs are converted into 2014 dollars using the Chemical Engineering Plant Cost Index (Chemical Engineering Magazine, 2012).

The total plant costs, TPC, are calculated by adding the indirect costs (engineering, contingency, startup, royalties, fees, and spare parts), ICs, to the total direct cost (Kreutz et al., 2008). The indirect costs are assumed to be 32% of the total direct costs. The production costs of the refinery are levelized in order to adequately compare alternative WTL technologies. The capital charges (CC) are calculated by multiplying the levelized capital charge rate (LCCR) with the interest during construction factor (IDCF) and the total overnight capital, as shown in Eq. (22) (Kreutz et al., 2008):

$$CC = LCCR \cdot IDCF \cdot TPC \tag{22}$$

An LCCR value of 14.38%/yr and an IDCF value of 7.16%/yr (with an overall multiplier of 15.41%/yr) is used to convert the TPC into a

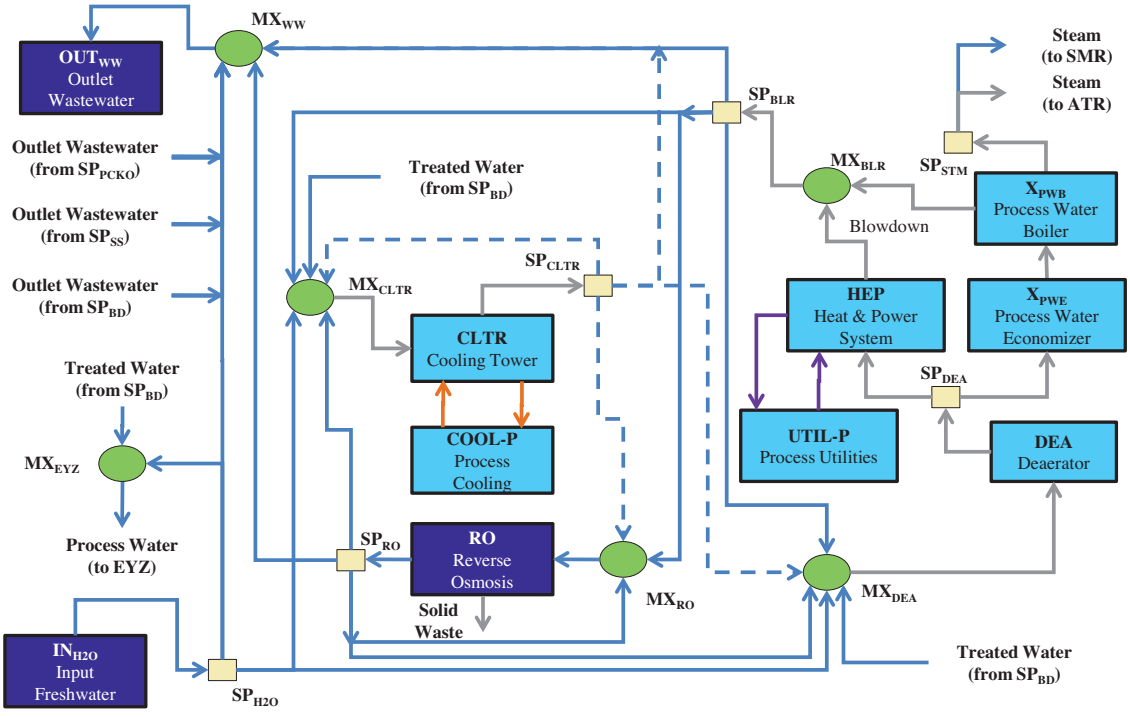

Fig. 12. Utility wastewater treatment section.

capital charge rate (Kreutz et al., 2008). Under the assumption of an operating capacity, CAP, of 330 days/yr and operating/maintenance, OM, costs of 4.5% of the TPC, the total levelized costs of a unit ($Cost^U$) is calculated using Eq. (23):

$$Cost_u^U = \left(\frac{LCCR \cdot IDCF}{CAP} + \frac{OM}{365}\right) \cdot \left(\frac{TPC_u}{Prod}\right) \quad (23)$$

Eq. (23) uses the total energy of products produced (Prod) to levelize the unit cost.

2.8. Objective function

The objective function shown in Eq. (24) is minimized to determine the lowest cost of a WTL refinery:

$$\text{MIN} \quad Cost_{MSW}^F + Cost_{H_2O}^F + Cost_{But}^F + Cost^{El} + Cost^{Seq} - Sales^{LPG} + \sum_{u \in U_{Inv}} Cost_u^U \quad (24)$$

Eq. (24) includes the feedstock costs ($Cost_{MSW}^F$, $Cost_{H_2O}^F$, & $Cost_{But}^F$), CO_2 sequestration cost ($Cost^{Seq}$), levelized investment cost ($Cost^U$), electricity cost ($Cost^{El}$), and profit obtained from the sale of byproduct LPG ($Sales^{LPG}$). The authors note that the electricity cost is positive if the WTL refinery inputs electricity and negative if the WTL refinery produces electricity. The terms in Eq. (24) are normalized with respect to the total energy of products produced. Other normalization factors (total volume of products, etc.) and other objective functions (maximizing net present value, etc.) can be incorporated into the MINLP model.

The large-scale non-convex mixed-integer non-linear optimization (MINLP) model described in the previous sections contains 15,568 continuous variables, 31 binary variables, 19,433 constraints, and 622 non-convex terms. The non-convex terms consist of 559 bilinear terms, 1 trilinear term, 3 quadrilinear terms, and 59 power functions. A branch-and-bound global optimization algorithm is used to solve the process synthesis model to global optimality (Baliban et al., 2012a). A mixed-integer linear relaxation is solved at each node via CPLEX (CPLEX, 2009). The non-linear equations are replaced by their linear relaxations, which are formed by using a piecewise-linear partitioning scheme that utilizes binary variables which are logarithmically dependent on the number of pieces to be partitioned. A distinct set of initial points (250 for the root node, 10 for all others) are generated using the solution pool feature of CPLEX. At each initial point, the binary variables are fixed and CONOPT is called to solve the nonlinear optimization model (NLP) (Drud, 1985). If the solution of the NLP is lower than the current solution, the upper bound is updated. If a node has a lower bound within ϵ of the current best upper bound ($(LB_{node}/UB) \geq 1-\epsilon$), that node is eliminated from the branch-and-bound tree. The reader is directed to optimization textbooks by Floudas (Floudas, 1995, 2000) and reviews of global optimization methods (Floudas and Pardalos, 1995; Floudas et al., 2005; Floudas and Gounaris, 2009) for a more detailed explanation of branch-and-bound algorithms. The reader is directed to work previously presented by Baliban et al. (2012a), for a more comprehensive description of the global optimization framework.

3. Computational studies

The process synthesis framework is used to examine the production of liquid transportation fuels from municipal solid waste. Twelve case studies illustrate the MINLP model described previously. The global optimization framework was terminated if all nodes in the branch-and-bound tree were processed or if 100 CPU hours had passed (Baliban et al., 2012a). Three sets of case studies examine the production of different ratios of products: (a) an unrestricted (U) fuel output, (b) maximization of diesel (D), and (c) commensurate with 2014 United States demand (R) (i.e., 67 vol% gasoline, 22 vol% diesel, 11 vol% kerosene) (Energy Information Administration, 2013). Each case study will examine four different refinery scales (1, 2, 5, and 10 thousand barrels per day) to illustrate the effects of refinery capacity. The WTL refinery capacities were chosen such that a feasible amount of MSW could be economically transported to the plant gate each day. The production output from the WTL refinery is expressed in terms of gasoline equivalent (based on the lower heating value of gasoline) so that the normalization constant in the denominator of the objective is constant. The case studies are denoted as $N-C$, where N represents the fuel composition of the products (U – Unrestricted, D – Diesel, R – U.S. Ratios) and C represents the refinery capacity (in kBD). Thus, U-2 represents a WTL refinery that outputs 2000 barrels per day (of gasoline equivalent) of unrestricted liquid fuels products.

Table 4
Cost parameters (2014 $) for the WTL refinery (Baliban et al., 2012c; Energy Information Administration, 2014; New York State Department of Environmental Conservation, 1990).

Item	Cost	Item	Cost
MSW	$0.00/dry metric ton MSW	RDF operation	$66.67/dry metric ton RDF
Butanes	$1.84/gallon	Propanes	$1.65/gallon
Electricity	$0.07/kWh	CO_2 TS&M[a]	$5/metric ton
Freshwater	$0.50/metric ton		

[a] Transportation, storage, and monitoring.

A constraint is included within the MINLP model that imposes at least a 50% reduction in GHG emissions from conventional fossil-fuel based processes. The typical GHG levels for a petroleum-based refinery and a natural gas combined cycle plant that produces electricity are 91.6 kg CO_{2eq}/GJ_{LHV} and 101.3 kg CO_{2eq}/GJ, respectively (Larson et al., 2009b; National Energy Technology Laboratory, 2007). The calculation of the GHG emissions for the natural gas combined cycle plant does not include carbon capture and sequestration (National Energy Technology Laboratory, 2007). If the WTL refinery inputs electricity, then the GHG emissions associated with electricity production are added to the life-cycle greenhouse gas emissions. Otherwise, the GHG emissions associated with electricity production are subtracted from the life-cycle GHG emissions of the WTL refinery.

The WTL cost parameters are shown in Table 4. The feedstock costs (MSW, butanes, and freshwater) include the costs for delivery to the plant gate, whereas the transportation costs for the products (i.e., electricity and propane) are not included in the product costs. As noted in Section 1, the negative cost associated with MSW make it an attractive precursor to liquid fuels and electricity. In the twelve case studies examined, it is assumed that the tipping fee received from the handling and disposal of MSW is equal to the transportation costs needed to deliver the feedstock to the plant gate. Therefore, the cost shown in Table 4 is $0.00/dry metric ton. The authors note that this is an overestimate on the price of MSW and the effects on the tipping fee will be examined later in the study. The costs associated with the operation of the RDF facility are based on the amount of RDF processed through the facility. The operation costs are assumed to be $30.00/wet metric ton of RDF (in 1990 dollars) and are taken from the Generic Technology Assessment Solid Waste Management Report (New York State Department of Environmental Conservation, 1990). These costs are converted to a dry basis (using a moisture content of 28 wt%), converted to 2014 dollars, and are shown in Table 4. The CO_2 capture and compression costs are included in the investment costs of the plant, while

Table 5
Topological information for the optimal solutions for the 12 case studies is shown. Municipal solid waste conversion (MSW Conv.) is gasification with a solid (S) or solid/vapor (S/V) fueled system. Temperatures (Temp.; °C) of the MSW gasifiers, along with the operating temperature of the forward or reverse water-gas-shift reactor, are shown. The presence of a gas turbine (GT) or a CO_2 sequestration system (CO2SEQ) is noted using yes (Y) or no (–). The FT units will be designated as either cobalt-based or iron-based. The FT hydrocarbons will be upgraded using fractionation (Fract.) or ZSM-5 catalytic conversion. Methanol conversion using methanol-to-gasoline (MTG) and methanol-to-olefins/olefins-to-gasoline-and-diesel (MTO/MOGD) is noted using yes (Y) or no (–).

Case study	U-1	U-2	U-5	U-10	D-1	D-2	D-5	D-10	R-1	R-2	R-5	R-10
MSW Conv.	S/V	S/V	S/V	S/V	S/V	S/V	S/V	S/V	S/V	S/V	S/V	S/V
MSW Temp.	800	850	800	800	800	800	850	800	850	850	800	850
WGS/RGS Temp.	300	300	300	300	–	300	300	300	300	300	300	300
Min Wax FT	–	–	–	–	–	–	–	–	–	–	–	–
Nom. Wax FT	–	–	–	–	–	–	–	–	–	–	–	–
FT Upgrading	–	–	–	–	–	–	–	–	–	–	–	–
MTG Usage	Y	Y	Y	Y	–	–	–	–	–	–	Y	Y
MTOD Usage	–	–	–	–	Y	Y	Y	Y	Y	Y	Y	Y
CO2SEQ Usage	–	–	–	–	–	–	–	–	–	–	–	–
GT Usage	–	–	–	–	–	–	–	–	–	–	–	–

the costs for the transportation, storage, and monitoring of CO_2 are shown in Table 4 (Baliban et al., 2012c).

The minimum number of heat exchanger matches for the optimal process topology need the following specifications: (i) the fluid flow rates and operating conditions of the heat engine, (ii) the amount of electricity produced by the heat engines, (iii) the amount of cooling water required by the heat engines, and (iv) the location of all pinch points in the subnetworks (Floudas, 1995; Floudas et al., 1986; Baliban et al., 2011, 2012b). These specifications are obtained once the global optimization framework has finished. The minimum annualized cost of the heat exchanger is then calculated after the minimum number of heat exchanger matches model. The reader is directed to works by Floudas et al. (Floudas, 1995; Floudas et al., 1986) and Elia et al. (Elia et al., 2010), for a more detailed description of the heat exchanger network. The investment cost of the heat exchanger network is then added to the overall WTL refinery investment cost (Baliban et al., 2012c).

3.1. Optimal process topologies

The optimal process topologies selected within the WTL refinery for the twelve case studies are shown in Table 5. Table 5 illustrates (i) the operation of the MSW gasifier, (ii) the temperature of the MSW gasifier, (iii) the selection of a forward or reverse WGS reactor, (iv) the synthesis gas conversion units, (v) the FT upgrading routes, (vi) the selection of a gas turbine, and (vii) the selection of a CO_2 sequestration system. The municipal solid waste gasifier can convert either solid MSW or a combination of solid MSW and recycle gases into synthesis gas. Each of the twelve case studies selected a gasifier with recycle feed and solid gas conversion. By utilizing a combination of solid/vapor fuel into the gasifiers, the refinery can convert some of the produced CO_2 into additional syngas.

Three possible temperatures (800 °C, 850 °C, or 900 °C) were considered for the operation of the MSW gasifier. The MSW gasifier was selected to be 800 °C in all of the case studies except for U-2, D-5, R-1, R-2, and R-10. Gasifiers operating at lower temperatures require less oxygen and therefore reduce the steam and electricity requirements of the refinery. However, these units produce less waste heat from syngas cooling. Additionally, because the equilibrium constant of the forward water-gas-shift reaction is larger at lower temperatures, these gasifiers have less favorable conditions for CO_2 consumption. At higher temperatures, the MSW gasifiers require more oxygen, but have more favorable conditions for CO_2 consumption.

Four temperatures (300 °C, 400 °C, 500 °C, or 600 °C) were considered for the operation of the dedicated water-gas-shift reactor. Each of the case studies, except for D-1, utilized a dedicated WGS unit operating at 300 °C that increased the H_2/CO ratio of the synthesis gas for hydrocarbon production at the expense of producing more CO_2.

Table 5 shows that the selection of the synthesis gas conversion technology depends heavily on the type of liquid fuels produced. In the unrestricted case studies, the syngas was converted into methanol and subsequently the methanol was converted into gasoline and LPG using MTG technology. The MTG route has lower investment costs than the FT routes. For the maximization of diesel case studies, the optimal topology was methanol-to-olefins (MTO) followed by olefins-to-gasoline/distillate (MOGD) technologies. The case studies that produced liquid fuels commensurate with U.S. demand utilized MTO/MOGD technologies for the 1 kBD and 2 kBD scales. Depending on which mode it operates in, the MOGD reactor can produce various ratios of gasoline, diesel, and kerosene that can satisfy U.S. demand. At 5 kBD, a topological shift is observed and both the MTO/MOGD and MTG technologies are utilized to produce the liquid fuels. The MTG unit will produce LPG and most of the gasoline, while the kerosene and diesel will be produced by the MOGD reactor.

CO_2 sequestration was not needed to meet the 50% reduction requirement from petroleum based processes in any of the twelve case studies. Additionally, none of the case studies selected a gas turbine. Instead, the light gases generated within the WTL refinery were sent to the fuel combustor and the autothermal reformer. The fuel combustor provides the heat necessary for various process units in the refinery. The reformed gases from the autothermal reformer were recycled back into the MSW gasifiers.

3.2. Overall costs of liquid fuels

The overall cost results for the twelve case studies is shown in Table 6. Each of the terms in Table 6 is normalized with respect to the total energy (GJ) of products produced in the WTL refinery. The total cost is calculated by summing the contributions from the feedstock costs, the CO_2 sequestration cost, the investment cost, the operating and maintenance costs, the electricity costs, and LPG profits. A negative value for electricity represents a WTL refinery that outputs electricity. Additionally, the break-even oil price (BEOP) is illustrated and calculated using the refiner's margin (Kreutz et al., 2008; Baliban et al., 2011). The BEOP represents the price at which the WTL refinery becomes competitive with petroleum-based processes. The lower bound and the optimality gap is calculated for each of the case studies.

The largest contributor to the total cost comes from the capital investment, which includes the capital charges and the O&M costs. A significant economy of scale is expected when comparing the 1 kBD and 10 kBD scales since a singular train is needed for most sections of these plants. Therefore, the refineries can take

advantage of the low scaling factor (between 0.5 and 0.7) associated with the different technologies since only one or two units are required to produce the desired amount of fuels. The benefits associated with economies of scale will dwindle above 10 kBD since these refineries will require multiple units in order to produce the desired quantity of fuels and the scaling factor for these units will approach 0.9 (Kreutz et al., 2008). Due to municipal solid waste availability and transportation concerns, scales above 10 kBD are not investigated in this paper.

The total investment cost represents between 62 and 64% of the total cost in the unrestricted case studies, 55–58% in the max diesel case studies, and 55–60% in the U.S. ratios case studies. As the refinery scale grew to 10 kBD, each of the refineries produced and sold electricity to the grid. There is no cost associated with MSW since it is assumed that the cost of transporting the feedstock to the plant gate is exactly equal to the tipping fee. It is noteworthy to point out the large cost associated with the operation of the RDF facility, which converts the MSW into a higher-calorific fuel. The RDF operation cost represents between 20 and 43% of the total cost in the unrestricted case studies, 18–36% in the max diesel case studies, and 18–39% in the U.S. ratios case studies.

The lowest overall cost was exhibited in the case studies that placed no restriction on the output composition of the liquid products. In these case studies, the optimal technology selected is the MTG reactor. The unrestricted case studies produced gasoline and LPG; the LPG generated provided additional economic incentive for the refinery. The next lowest cost of fuels production was from the case studies that produced liquid fuels in ratios consistent with U.S. demand. At scales above 5 kBD, the optimal technology included methanol-to-gasoline and methanol-to-olefins/olefins-to-gasoline-and-distillate. The max diesel case studies had the highest overall cost of liquid fuels production. The optimal technology selected was the MTO and MOGD reactors. The lower costs associated with the R-1 and R-2 case studies, when compared to the D-1 and D-2 case studies, is due to the slightly smaller flowrates of feedstock required in the former cases. The smaller flowrate will lead to smaller units that ultimately reduce the capital charges. The BEOP ranges from $117/bbl–$123/bbl for a 1 kBD plant, $96/bbl–$100/bbl for a 2 kBD plant, $73/bbl–$83/bbl for a 5 kBD plant, and $61/bbl–$67/GJ/bbl for a 10 kBD plant. The optimality gap for the case studies ranges between 1 and 8%.

3.3. Parametric analysis

The BEOP calculated in Table 6 is based on a MSW delivered price of $0.00/dry ton. In this section, the effect of the tipping fee on the overall cost of liquid fuels production for the unrestricted case studies is examined. The BEOP is calculated for the U-1, U-2, U-5, and U-10 case studies assuming that the delivered MSW price (Transportation – Tipping Fee) is priced from $0.00 to −$35.00 per dry ton. The results are plotted in Fig. 13.

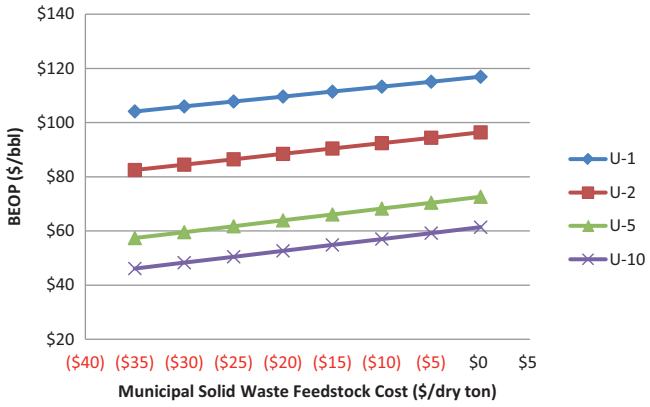

Fig. 13. Parametric analysis of the municipal solid waste cost. The break-even oil price (BEOP) is plotted for the case studies with an unrestricted product composition.

Fig. 13 illustrates that when the MSW delivered price is as low as −$35.00/dry ton, the break even oil price for the U-1 case decreases to $105/bbl. Similarly, the BEOP for U-2 and U-5 refineries reduce to $83/bbl and $58/bbl, respectively, when the MSW delivered price is −$35.00/dry ton. For a similar MSW delivered price, the BEOP price decreases to $47/bbl for a U-10 refinery. This represents a 24% decrease in the break even oil price from the nominal value shown in Table 6. Thus, Fig. 13 illustrates that the tipping fee can make the economics of a WTL refinery significantly more attractive.

3.4. Investment costs

The total plant costs (TPC) and the breakdown for the major sections of the WTL refinery for the twelve case studies are shown in Table 7. The major sections of the WTL refinery include: syngas generation, syngas cleaning, hydrocarbon production, hydrocarbon upgrading, hydrogen/oxygen production, heat and power integration, and wastewater treatment. The syngas generation section contributes the largest portion toward the total plant cost and represents between 42 and 50% of the TPC for the twelve case studies. The syngas generation section includes the costs for the RDF facility, as well as the cost associated with the MSW gasifiers. Syngas cleaning is the second largest contributor to the TPC and represents between 17 and 21% of the total plant cost. The syngas cleaning section includes costs associated with the dedicated water-gas-shift reactor and CO_2 capture and compression. The third and fourth

Table 6
Overall cost results for the 12 case studies. The contribution to the total costs (in $/GJ) comes from MSW, butane, water, CO_2 transportation/storage/monitoring (CO_2 TS&M), investment, input electricity, and operations/maintenance (O&M). LPG and output electricity are allowable byproducts (negative value). The overall costs, as well as the lower bound values, are reported and the optimality gap between the optimal solution and the lower bound is shown.

Contribution to cost ($/GJ of products)	U-1	U-2	U-5	U-10	D-1	D-2	D-5	D-10	R-1	R-2	R-5	R-10
Municipal solid waste	0.00	0.00	0.00	0.00	0.00	0.00	0.00	0.00	0.00	0.00	0.00	0.00
RDF operation	4.80	5.23	5.73	5.73	4.46	4.35	5.47	5.28	4.33	4.33	5.14	5.59
Butane	0.00	0.00	0.00	0.00	0.00	0.00	0.00	0.00	0.00	0.00	0.00	0.00
Water	0.01	0.01	0.02	0.02	0.02	0.01	0.02	0.02	0.01	0.01	0.01	0.02
CO_2 TS&M	0.00	0.00	0.00	0.00	0.00	0.00	0.00	0.00	0.00	0.00	0.00	0.00
Investment	14.95	12.76	10.00	8.39	14.36	11.21	10.02	7.90	14.05	11.19	9.76	8.51
O&M	3.95	3.37	2.64	2.21	3.79	2.96	2.65	2.09	3.71	2.95	2.58	2.25
Electricity	2.19	0.81	−0.54	−0.54	2.03	1.94	−0.85	−0.79	1.94	1.93	0.42	−0.73
LPG	−2.34	−2.34	−2.34	−2.34	0.00	0.00	0.00	0.00	0.00	0.00	−1.42	−1.42
Total ($/GJ)	23.56	19.83	15.51	13.47	24.67	20.47	17.31	14.49	24.05	20.42	16.49	14.21
Total ($/bbl)	116.90	96.38	72.61	61.36	123.01	99.90	82.52	66.99	119.58	99.61	77.98	65.45
Lower bound ($/GJ)	23.32	19.60	15.11	13.30	24.39	20.16	15.91	14.31	22.85	19.76	16.31	14.06
Gap (%)	1.03	1.15	2.59	1.28	1.13	1.52	8.13	1.27	5.00	3.25	1.08	1.07

Table 7
The costs of the syngas generation, syngas cleaning, hydrocarbon production, hydrocarbon upgrading, hydrogen/oxygen production, heat and power integration, and wastewater treatment sections of the WTL refinery are shown. All values are shown in MM$ and are also expressed in $/bpd by dividing the total investment cost by the total plant capacity.

Contribution to cost (MM $)	U-1	U-2	U-5	U-10	D-1	D-2	D-5	D-10	R-1	R-2	R-5	R-10
Syngas generation	75	131	269	490	72	115	262	452	69	115	251	477
Syngas cleaning	38	59	108	168	35	55	109	157	35	55	104	164
Hydrocarbon production	18	27	48	75	17	25	43	73	16	25	48	74
Hydrocarbon upgrading	27	42	77	121	26	41	75	118	26	41	97	151
Hydrogen/oxygen production	11	16	26	37	11	16	36	35	11	16	25	38
Heat and power integration	2	16	44	69	1	2	46	69	2	2	33	70
Wastewater treatment	6	10	19	29	7	10	20	29	6	10	18	29
Total (MM $)	176	301	590	989	169	264	591	932	166	264	575	1003
Total ($/bpd)	176,239	150,407	117,946	98,896	185,952	145,108	129,755	102,315	171,948	136,474	119,104	103,786

largest contributors to the TPC include the hydrocarbon upgrading and hydrocarbon production sections, respectively. The hydrocarbon upgrading section includes the methanol conversion units and all units associated with the FT hydrocarbon upgrading route. The hydrocarbon production section includes costs associated with the methanol synthesis reactor and the FT units. The full breakdown of the major sections is shown in Table 7. The "overnight" cost can be calculated from the total plant cost by factoring in the preproduction costs, inventory capital, financing costs, and other owner's costs (Kreutz et al., 2008; National Energy Technology Laboratory, 2007).

The total plant cost ranges between $166 and $176 MM for 1 kBD plants, $264–$301 MM for 2 kBD plants, $575–$591 MM for 5 kBD plants, and $932–$1003 MM for 10 kBD plants. To illustrate the economies of scale, the normalized cost of production is calculated by dividing the TPC by the production capacity of the WTL refinery. For example, when scaling the refinery from 1 kBD to 10 kBD, the normalized capital cost decreases between 40 and 45%.

3.5. Material and energy balances

Material balances for the twelve cases studies utilizing municipal solid waste are shown in Table 8. RDF is shown in dry tons per hour (dt/h). Butane, water, gasoline, diesel, kerosene, and LPG are shown in thousand barrels per day (kBD). The amount of sequestered and vented CO_2 is also shown in tons per hour. The unrestricted case studies only produce gasoline and LPG. The case studies that maximize the production of diesel produce all three liquid fuels products. The diesel product was equivalent to 75% of the total liquid product, while gasoline and kerosene were equivalent to 12% and 13% of the total liquid product, respectively. No byproduct LPG was produced in any of these case studies. The case studies that produced liquid fuels in ratios commensurate with U.S. demand showed a topological shift in the optimal process topology. At the 1 kBD and 2 kBD scales, no byproduct LPG was produced since the optimal topology was the MTO/MOGD technologies. At refinery scales larger than 5 kBD, MTG and MTO/MOGD were chosen as the optimal technologies. At these refinery scales, LPG was produced as a byproduct as a consequence of the inclusion of the MTG reactor. None of the CO_2 needed to be sequestered to meet the 50% reduction of greenhouse gas emissions from petroleum-based processes since municipal solid waste is considered a type of biomass.

The overall energy balances for the 12 case studies are shown in Table 9. MSW, butane, and electricity are the energy inputs into the system, while the liquid products, LPG, and electricity are the energy outputs. The values in Table 9 are expressed in MW and are based on the lower heating value of the component. If electricity is input into the system, it is denoted by a positive value in Table 9. The overall efficiency is calculated by dividing the sum of the energy outputs by the sum of the energy inputs. The unrestricted case studies have an efficiency that ranges from 65 to 72%, while the case studies that maximize the production of diesel and produce fuels that are commensurate with U.S. ratios have efficiencies that range between 62–67% and 64–67%, respectively.

3.6. Carbon and greenhouse gas balances

Table 10 illustrates the overall carbon balance (kg/s) for each of the 12 case studies. Carbon is input into the refinery by either MSW or butane and output as liquid product, LPG byproduct, vented CO_2, or sequestered CO_2. The amount of carbon input by any incoming air into the WTL is negligible and therefore neglected. The total carbon conversion is calculated by dividing the carbon of the products (gasoline, diesel, kerosene, LPG) by the incoming carbon. The overall carbon conversion ranges between 47 and 56% for the unrestricted case studies, 46–54% for the case studies that maximize the production of diesel, and 46–55% for the U.S. ratios case studies. The amount of carbon exiting as LPG is about 12% of that leaving as gasoline in the unrestricted case studies and about 7% of that leaving as gasoline, diesel, and kerosene in the R-5 and R-10 case studies.

The total greenhouse gas emissions (in kg CO_2 equivalent/s) for the major inputs and outputs of the WTL refineries are shown in Table 11. Each case study included a constraint that imposed at least a 50% reduction in the GHG emissions from conventional fossil-fuel based processes. The GHG emissions rates include (a) acquisition

Table 8
Overall material balance for the 12 case studies. The inputs to the WTL refinery are MSW, butane, and water, while the outputs include gasoline, diesel, kerosene, LPG, sequestered CO_2, and vented CO_2.

Material balances	U-1	U-2	U-5	U-10	D-1	D-2	D-5	D-10	R-1	R-2	R-5	R-10
RDF (dt/h)	16.52	35.98	98.62	197.22	15.35	29.97	94.18	181.74	14.91	29.82	88.40	192.54
Butane (kBD)	0.00	0.00	0.00	0.00	0.00	0.00	0.00	0.00	0.00	0.00	0.00	0.00
Water (kBD)	0.89	1.92	5.67	11.34	1.66	1.80	7.25	1.13	0.91	1.81	4.82	11.59
Gasoline (kBD)	1.00	2.00	5.00	10.00	0.11	0.22	0.56	1.12	0.65	1.30	3.25	6.49
Diesel (kBD)	0.00	0.00	0.00	0.00	0.68	1.37	3.41	6.83	0.21	0.42	1.04	2.08
Kerosene (kBD)	0.00	0.00	0.00	0.00	0.12	0.23	0.58	1.15	0.11	0.22	0.54	1.09
LPG (kBD)	0.19	0.37	0.93	1.86	0.00	0.00	0.00	0.00	0.00	0.00	0.56	1.13
Seq. CO_2 (tons/h)	0.00	0.00	0.00	0.00	0.00	0.00	0.00	0.00	0.00	0.00	0.00	0.00
Vented CO_2 (tons/h)	13.93	33.46	100.15	200.26	13.50	25.59	100.69	188.76	12.80	25.59	84.46	198.91

Table 9
Overall energy balance for the 12 case studies. The energy inputs are MSW, butane, or electricity; while the energy outputs are gasoline, diesel, kerosene, LPG, or electricity. Electricity is denoted as a positive value if it is input into the system and as a negative value if it is output from the system.

Energy balances (MW)	U-1	U-2	U-5	U-10	D-1	D-2	D-5	D-10	R-1	R-2	R-5	R-10
RDF	97.78	212.95	583.66	1167.20	90.87	177.36	557.39	1075.59	88.24	176.47	523.19	1139.49
Butane	0.00	0.00	0.00	0.00	0.00	0.00	0.00	0.00	0.00	0.00	0.00	0.00
Gasoline	63.72	127.44	318.59	637.18	7.15	14.30	35.74	71.49	41.38	82.75	206.88	413.76
Diesel	0.00	0.00	0.00	0.00	48.58	97.15	242.88	485.76	14.81	29.62	74.05	148.10
Kerosene	0.00	0.00	0.00	0.00	7.99	15.99	39.97	79.93	7.53	15.06	37.66	75.31
LPG	11.33	22.66	56.65	113.31	0.00	0.00	0.00	0.00	0.00	0.00	34.30	68.59
Electricity	7.19	5.29	−8.82	−17.65	6.65	12.69	−13.93	−26.00	6.35	12.66	6.86	−23.96
Efficiency (%)	71.5	68.8	65.8	65.8	65.3	67.1	59.7	61.7	67.4	67.4	66.6	64.0

Table 10
Carbon accounting (in kg/s) is shown for the 12 case studies. MSW and butane are the carbon inputs, while the carbon outputs are the liquid products, LPG byproduct, vented CO_2, or sequestered (Seq.) CO_2. The overall carbon conversion for each case study is also calculated and shown.

Carbon balances (kg/s)	U-1	U-2	U-5	U-10	D-1	D-2	D-5	D-10	R-1	R-2	R-5	R-10
RDF	2.38	5.18	14.19	28.38	2.21	4.31	13.55	26.15	2.15	4.29	12.72	27.71
Butane	0.00	0.00	0.00	0.00	0.00	0.00	0.00	0.00	0.00	0.00	0.00	0.00
Gasoline	1.19	2.38	5.84	11.88	0.13	0.26	0.66	1.32	0.77	1.53	3.85	7.71
Diesel	0.00	0.00	0.00	0.00	0.92	1.83	4.58	9.15	0.28	0.56	1.40	2.79
Kerosene	0.00	0.00	0.00	0.00	0.14	0.29	0.72	1.44	0.14	0.27	0.68	1.35
LPG	0.14	0.28	0.70	1.40	0.00	0.00	0.00	0.00	0.00	0.00	0.42	0.85
Vented CO_2	1.06	2.54	7.59	15.18	1.02	1.94	7.63	14.31	0.97	1.94	6.40	15.08
Seq. CO_2	0.00	0.00	0.00	0.00	0.00	0.00	0.00	0.00	0.00	0.00	0.00	0.00
Conversion (%)	55.82	51.26	46.05	46.76	53.90	55.24	43.94	45.54	55.00	55.01	49.91	45.83

Table 11
The greenhouse gas (GHG) balances for the 12 case studies are shown. The total GHG emissions (in CO_2 equivalents – kg CO_2 eq/s), as well as the GHG emissions avoided from liquids production (GHGAF), emissions due to electricity usage (GHGAE), and overall GHG emissions (LGHG), are also illustrated.

GHG balances (kg CO_2 eq/s)	U-1	U-2	U-5	U-10	D-1	D-2	D-5	D-10	R-1	R-2	R-5	R-10
RDF	−7.98	−17.39	−47.66	−95.30	−7.42	−14.48	−45.51	−87.82	−7.21	−14.41	−42.72	−93.04
Butane	0.00	0.00	0.00	0.00	0.00	0.00	0.00	0.00	0.00	0.00	0.00	0.00
Gasoline	4.27	8.56	21.39	42.78	0.48	0.96	2.40	4.80	2.78	5.56	13.89	27.78
Diesel	0.00	0.00	0.00	0.00	3.33	6.65	16.63	33.25	1.01	2.03	5.07	10.14
Kerosene	0.00	0.00	0.00	0.00	0.53	1.06	2.64	5.28	0.50	0.99	2.49	4.97
LPG	0.52	1.04	2.61	5.21	0.00	0.00	0.00	0.00	0.00	0.00	1.58	3.15
Vented CO_2	3.87	9.29	27.82	55.63	3.75	7.11	27.97	52.43	3.56	7.11	23.46	55.25
Seq. CO_2	0.00	0.00	0.00	0.00	0.00	0.00	0.00	0.00	0.00	0.00	0.00	0.00
LGHG	0.68	1.50	4.16	8.32	0.66	1.29	4.12	7.94	0.64	1.28	3.76	8.26
GHGAF	6.87	13.75	34.37	68.74	5.84	11.67	29.18	58.37	5.84	11.67	32.32	64.65
GHGAE	−0.73	−0.54	0.89	1.79	−0.67	−1.29	1.41	2.63	−0.64	−1.28	−0.69	2.43
GHGI	0.11	0.11	0.12	0.12	0.13	0.12	0.13	0.13	0.12	0.12	0.12	0.12

and transportation of the MSW and butane feeds, (b) transportation and use of the liquid products and LPG, (c) transportation and sequestration of CO_2, (d) venting of CO_2, and (e) atmospheric sequestration of CO_2 during growth of biomass (present in MSW) due to photosynthesis or sequestration. The well-to-wheel emissions for the WTL refinery are computed by calculating the GHG emissions from (a) to (e) and assuming transportation distances of 50 miles for feedstocks, 100 miles for products, and 50 miles for CO_2. The total lifecycle GHG emissions (LGHG) is illustrated in Table 11.

The total greenhouse gas emissions avoided from liquid fuels (GHGAF) is equivalent to the total energy of fuels produced multiplied by a typical petroleum-based emissions level (i.e., 91.6 kg CO_{2eq}/GJ_{LHV}). The GHG emissions avoided from electricity (GHGAE) is equivalent to the total energy of electricity input or output into a refinery multiplied by a typical natural gas-based emissions level (i.e., 101.3 kg CO_{2eq}/GJ). A negative value of GHGAE represents electricity that is input into the refinery, while a positive value indicates electricity that is output from the refinery. The GHG index (GHGI) is calculated by dividing the LGHG by the summation of GHGAF and GHGAE. GHGI values less than 1 are indicative of processes that have superior life-cycle GHG emissions than fossil-fuel based processes. As shown in Table 11, the GHGI value for the 12 case studies is between 0.11 and 0.13. These values represent refineries that reduce lifecycle emissions between 87 and 89% from petroleum-based processes.

4. Conclusions

This paper is the first that investigates the conversion of municipal solid waste into gasoline, diesel, and kerosene by analyzing multiple hydrocarbon production and upgrading technologies. A process synthesis framework that includes simultaneous heat, power, and water integration is utilized to investigate the thermochemical conversion of municipal solid waste into liquid transportation fuels. Twelve case studies were presented that compared three different product ratios (unrestricted fuels composition, maximization of diesel product, U.S. ratios) at four unique refinery scales. A global optimization branch-and-bound framework was utilized to determine the optimal process topology for each of the twelve case studies. The solution of the MINLP model was theoretically guaranteed to be less than 8% of the best possible value.

Because of the tipping fee received while disposing of municipal solid waste, the results illustrated in this paper become very competitive with petroleum-based processes. The overall cost of unrestricted liquid fuels productions is $117/bbl for a 1 kBD plant, $96/bbl for a 2 kBD plant, $73/bbl for a 5 kBD plant, and $61/bbl for a 10 kBD plant. For refineries that maximize production of diesel,

the break-even oil price is $123/bbl for a 1 kBD plant, $100/bbl for a 2 kBD plant, $83/bbl for a 5 kBD plant, and $67/bbl for a 10 kBD plant. For the U.S. ratios case studies, the break-even oil price is $120/bbl for a 1 kBD plant, $100/bbl for a 2 kBD plant, $78/bbl for a 5 kBD plant, and $65/bbl for a 10 kBD plant. Moreover, these results are for an MSW delivered price of $0.00/dry ton, which is an overestimate on the price of MSW since tipping fees in the U.S. can be as high as $70.00/dry ton. For an MSW delivered price of −$35.00/dry ton, the break-even oil price for a U-10 plant decreases to $47/bbl. Additionally, a complete parametric analysis of the municipal solid waste price was presented. The results show that a refinery utilizing municipal solid waste can become economically competitive with petroleum-based processes while significantly reducing life-cycle GHG emissions.

Acknowledgments

The authors acknowledge partial financial support from the National Science Foundation (NSF EFRI-0937706 and NSF CBET-1158849) and the Andlinger Center for Energy and Environment.

Appendix A. Supplementary data

Supplementary data associated with this article can be found, in the online version, at http://dx.doi.org/10.1016/j.compchemeng.2014.10.007.

References

Ahmetovic E, Grossmann IE. Global superstructure optimization for the design of integrated process water networks. AIChE J 2010a;57:434–57.
Ahmetovic E, Grossmann IE. Optimization of energy and water consumption in corn-based ethanol plants. Ind Eng Chem Res 2010b;49:7972–82.
Baliban RC, Elia JA, Floudas CA. Toward novel biomass, coal, and natural gas processes for satisfying current transportation fuel demands. 1. Process alternatives, gasification modeling, process simulation, and economic analysis. Ind Eng Chem Res 2010;49:7343–70.
Baliban RC, Elia JA, Floudas CA. Optimization framework for the simultaneous process synthesis, heat and power integration of a thermochemical hybrid biomass, coal, and natural gas facility. Comp Chem Eng 2011;35:1647–90.
Baliban RC, Elia JA, Misener R, Floudas CA. Global optimization of a MINLP process synthesis model for thermochemical based conversion of hybrid coal, biomass, and natural gas to liquid fuels. Comp Chem Eng 2012a;42:64–86.
Baliban RC, Elia JA, Floudas CA. Simultaneous process synthesis, heat, power, and water integration of thermochemical hybrid biomass, coal, and natural gas facilities. Comp Chem Eng 2012b;37:297–327.
Baliban RC, Elia JA, Weekman VW, Floudas CA. Process synthesis of hybrid coal, biomass, and natural gas to liquids via Fischer–Tropsch synthesis, ZSM-5 catalytic conversion, methanol synthesis, methanol-to-gasoline, and methanol-to-olefins/distillate technologies. Comp Chem Eng 2012c;47:29–56.
Baliban RC, Elia JA, Floudas CA, Xiao X, Zhang Z, Li J, et al. Thermochemical conversion of duckweed biomass to gasoline, diesel, and jet fuel: process synthesis and global optimization. Ind Eng Chem Res 2013a:11436–50.
Baliban RC, Elia JA, Floudas CA. Novel natural gas to liquids (GTL) technologies: process synthesis and global optimization strategies. AIChE J 2013b;59:505–31.
Baliban RC, Elia JA, Floudas CA. Biomass and natural gas to liquid transportation fuels: process synthesis, global optimization, and topology analysis. Ind Eng Chem Res 2013c;52:3381–406.
Baliban RC, Elia JA, Floudas CA. Biomass to liquid transportation fuels (BTL) systems: process synthesis and global optimization framework. Energy Environ Sci 2013d;6:267–87.
Baliban RC, Elia JA, Floudas CA, Gurau B, Weingarten MB, Klotz SD. Hardwood biomass to gasoline, diesel, and jet fuel. 1. Process synthesis and global optimization of a thermochemical refinery. Energy Fuels 2013e;27:4302–24.
Balmer P, Mattsson B. Wastewater treatment plant operation costs. Water Sci Technol 1994;30:7–15.
Bechtel. Baseline design/economics for advanced Fischer–Tropsch Technology. Contract No. DE-AC22-91PC90027; 1992.
Bechtel. Aspen Process flowsheet simulation model of a Battelle biomass-based gasification, Fischer–Tropsch liquefaction and combined-cycle power plant. Contract Number: DE-AC22-93PC91029; 1998. http://www.fischer-tropsch.org/
Chemical Engineering Magazine. Chemical Engineering plant cost index; 2012. http://www.che.com/pci/
Choy KK, Porter JF, Hui C-W, McKay G. Process design and feasibility study for small scale MSW gasification. Chem Eng J 2004;105:31–41.
Christensen TH. Solid waste technology & management, vol. 2. Wiley Online Library; 2011.
CPLEX. ILOG CPLEX C++ API 12.1 reference manual; 2009.
de Klerk A. Fischer–Tropsch refining. Edison, NJ: Wiley-VCH Verlag & Co. KGaA; 2011.
Diaz LF, Savage GM, Golueke CG. Resource recovery from municipal solid wastes, vol. 1. Boca Raton, FL: CRC Press; 1982.
Drud A. CONOPT: a GRG code for large sparse dynamic nonlinear optimization problems. Math Program 1985;31:153–91.
Duran MA, Grossmann IE. Simultaneous optimization and heat integration of chemical processes. AIChE J 1986;32:123–38.
EIA. Methodology for allocating municipal solid waste to biogenic and non-biogenic energy; 2007. http://www.eia.gov/totalenergy/data/monthly/pdf/historical/msw.pdf
EIA. International Energy Statistics; 2012. http://www.eia.gov/countries/data.cfm
Elia JA, Floudas CA. Energy supply chain optimization of hybrid feedstock processes: a review. Annu Rev Chem Biomol Eng 2014;5:147–79.
Elia JA, Baliban RC, Floudas CA. Toward novel biomass, coal, and natural gas processes for satisfying current transportation fuel demands. 2. Simultaneous heat and power integration. Ind Eng Chem Res 2010;49:7371–88.
Energy Information Administration. Monthly energy review – July 2013. Document Number: DOE/EIA-0035(2013/07); 2013. http://www.eia.gov/totalenergy/data/monthly/archive/00351307.pdf
Energy Information Administration. Monthly energy review – May 2014. Document Number: DOE/EIA-0035(2014/05); 2014. http://www.eia.gov/totalenergy/data/monthly
EPA. Municipal solid waste generation, recycling and disposal in the United States: Facts and Figures for 2011. Document Number: EPA530-R-13-001; 2013. http://www.epa.gov/osw/nonhaz/municipal/pubs
European Commission – Directorate General Environment. Refuse derived fuel, current practice and perspectives; 2003.
Floudas CA, Gounaris CE. A review of recent advances in global optimization. J Global Optim 2009;45:3–38.
Floudas CA, Pardalos PM. State of the art in global optimization: computational methods and applications. J Global Optim 1995;7:113.
Floudas CA, Ciric AR, Grossmann IE. Automatic synthesis of optimum heat exchanger network configurations. AIChE J 1986;32:276–90.
Floudas CA, Akrotirianakis IG, Caratzoulas S, Meyer CA, Kallrath J. Global optimization in the 21st century: advances and challenges. Comp Chem Eng 2005;29:1185–202.
Floudas CA, Elia JA, Baliban RC. Hybrid and single feedstock energy processes for liquid transportation fuels: a critical review. Comp Chem Eng 2012;41:24–51.
Floudas CA. Nonlinear and mixed-integer optimization. New York: Oxford University Press; 1995.
Floudas CA. Deterministic global optimization: theory, methods and applications. Dordrecht, Netherlands: Kluwer Academic Publishers; 2000.
Gregor JH, Gosling CD, Fullerton HE. Upgrading Fischer–Tropsch LPG with the cyclar process. Contract No. DE-AC22-86PC90014; 1989.
Grossmann IE, Martín M. Energy and water optimization in biofuel plants. Chin J Chem Eng 2010;18:914–22.
He M, Xiao B, Liu S, Guo X, Luo S, Xu Z, et al. Hydrogen-rich gas from catalytic steam gasification of municipal solid waste (MSW): influence of steam to MSW ratios and weight hourly space velocity on gas production and composition. Int J Hydrogen Energy 2009;34:2174–83.
Jones SB, Zhu Y, Valkenburg C. Municipal solid waste (MSW) to liquid fuels synthesis. Vol. 2: A techno-economic evaluation of the production of mixed alcohols. Richland, WA: Pacific Northwest National Laboratory; 2009.
Karuppiah R, Grossmann IE. Global optimization for the synthesis of integrated water systems in chemical processes. Comput Chem Eng 2006;30:650–73.
Kreutz T, Williams R, Consonni S, Chiesa P. Co-production of hydrogen, electricity and CO_2 from coal with commercially ready technology. Part B: Economic analysis. Int J Hydrogen Energy 2005;30:769–84.
Kreutz TG, Larson ED, Liu G, Williams RH. Fischer–Tropsch fuels from coal and biomass. In: Proceedings of the 25th International Pittsburgh Coal Conference; 2008.
Krieth F. Handbook of solid waste management. New York, NY: McGraw-Hill, Inc; 1994.
Larson ED, Jin H, Celik FE. Large-scale gasification-based coproduction of fuels and electricity from switchgrass. Biofuels Bioprod Biorefin 2009a;3:174–94.
Larson ED, Fiorese G, Liu G, Williams RH, Kreutz TG, Consonni S. Co-production of decarbonized synfuels and electricity from coal + biomass with CO_2 capture and storage: an Illinois case study. Energy Environ Sci 2009b., http://dx.doi.org/10.1039/B911529C.
Liu DH, Lipták BG. Hazardous waste and solid. Boca Raton, FL: CRC Press; 1999.
Meyers RA. Handbook of petroleum refining processes. New York, NY: McGraw-Hill; 2003.
Michaels T. The 2010 ERC directory of waste-to-energy plants. Washington, D.C.: Energy Recovery Council; 2010.
Mobil Research and Development. Corporation, research guidance studies to assess gasoline from coal by methanol-to-gasoline and sasol-type Fischer–Tropsch Technologies. USDOE contract EF-77-C-01-2447; 1978.
Mobil Research and Development Corporation. Slurry Fischer–Tropsch/mobil two stage process of converting syngas to high octane gasoline. USDOE contract DE-AC22-80PC30022; 1983.
Mobil Research and Development Corporation. Two-stage process for conversion of synthesis gas to high quality transportation fuels. USDOE contract DE-AC22-83PC60019; 1985.

Mokrani T, Scurrell M. Gas conversion to liquid fuels and chemicals: the methanol route-catalysis and processes development. Catal Rev 2009;51:1–145.
National Energy Technology Laboratory. Cost and performance baseline for fossil energy plants. Volume 1: Bituminous coal and natural gas to electricity final report. Document Number: DOE/NETL-2007/1281; 2007. http://www.netl.doe.gov/energy-analyses/baseline_studies.html
National Renewable Energy Laboratory. Process design and economics for conversion of lignocellulosic biomass to ethanol: thermochemical pathway by indirect gasification and mixed alcohol synthesis. USDOE contract DE-AC36-08GO28308; 2011.
National Renewable Energy Laboratory. Gasoline from wood via integrated gasification, synthesis, and methanol-to-gasoline technologies. USDOE contract DE-AC36-08GO28308; 2011.
New York State Department of Environmental Conservation. Generic technology assessment solid waste management; 1990. http://www.dec.ny.gov/docs/materials_minerals_pdf/generictech1.pdf
Niziolek AM, Onel O, Elia JA, Baliban RC, Xiao X, Floudas CA. Coal and biomass to liquid transportation fuels: process synthesis and global optimization strategies. Ind Eng Chem Res 2014., http://dx.doi.org/10.1021/ie500505h [in press].
Onel O, Niziolek AM, Hasan M, Floudas CA. Municipal solid waste to liquid transportation fuels – Part I: Mathematical modeling of a municipal solid waste gasifier. Comput Chem Eng 2014., http://dx.doi.org/10.1016/j.compchemeng.2014.03.008 [in press].
Psomopoulos C, Bourka A, Themelis NJ. Waste-to-energy: a review of the status and benefits in USA. Waste Manage 2009;29:1718–24.
Ruth LA. Energy from municipal solid waste: a comparison with coal combustion technology. Prog Energy Combust Sci 1998;24:545–64.
Santibañez-Aguilar JE, Ponce-Ortega JM, Betzabe González-Campos J, Serna-González M, El-Halwagi MM. Optimal planning for the sustainable utilization of municipal solid waste. Waste Manage 2013;33:2607–22.
Stehlík P. Contribution to advances in waste-to-energy technologies. J Clean Prod 2009;17:919–31.
Steynberg A, Dry M. Fischer–Tropsch technology. Amsterdam, Netherlands: Elsevier; 2004.
Stubenberger G, Scharler R, Zahirovic S, Obernberger I. Experimental investigation of nitrogen species release from different solid biomass fuels as a basis for release models. Fuel 2008;87:793–806.
Tabak SA, Yurchak S. Conversion of methanol over ZSM-5 to fuels and chemicals. Catal Today 1990;6:307–27.
Tabak S, Krambeck F, Garwood W. Conversion of propylene and butylene over ZSM-5 catalyst. AIChE J 1986;32:1526–31.
Valkenburg C, Walton C, Thompson B, Gerber M, Jones S, Stevens D. Municipal solid waste (MSW) to liquid fuels synthesis. Vol. 1: Availability of feedstock and technology. Richland, WA: Pacific Northwest National Laboratory; 2009.
Warren A, El-Halwagi M. An economic study for the co-generation of liquid fuel and hydrogen from coal and municipal solid waste. Fuel Process Technol 1996;49:157–66.
White PR, Franke M, Hindle P. Integrated solid waste management: a lifecycle inventory. Edison, NJ: Wiley-Blackwell; 2001.
Zhou J. Simulation of fuel-bound nitrogen evolution in biomass gasification. In: Proceedings of the 32nd intersociety energy conversion engineering conference; 1997.